Revue de micropaléontologie 82 (2024) 100755

Contents lists available at ScienceDirect

Revue de micropaléontologie

journal homepage: www.elsevier.com/locate/revmic

Putting the dead to work: A new method to assess the autochthony of marine Ostracoda death assemblages

Giuseppe Aiello[a], Roberta Parisi[b,*], Ilaria Mazzini[b], Diana Barra[a,c]

[a] Dipartimento di Scienze della Terra, dell'Ambiente e delle Risorse, Federico II University of Naples, Via Vicinale Cupa Cintia, 21, 80126 Naples, Italy
[b] CNR - Institute of Environmental Geology and Geoengineering, Area della Ricerca di Roma 1, Via Salaria km 29,300, 00015 Montelibretti, RM, Italy
[c] Istituto Nazionale di Geofisica e Vulcanologia, Osservatorio Vesuviano, Via Diocleziano, 328, 80125 Naples, Italy

ARTICLE INFO

Keywords:
Population age structure
Benthic ostracods
Grain size
Development stages

ABSTRACT

Sedimentary and paleontological records can be powerful means of reconstructing ecological and physical environmental changes, by using a variety of records extending proxies to extend chronologies beyond the reach of instrumental or manual records. Ostracods are often used as paleoenvironmental proxies. Estimating the population age structure could be a useful tool for assessing the influence of some environmental parameters on death assemblages and for determining the autochthoneity or allochthoneity of the species that make up the thanatocoenosis. In the literature, several methods based on population age structure have been proposed to distinguish autochthonous and allochthonous components of life/death ostracod assemblages.

The Adult:Juveniles ratio analysis of a rich and well-preserved ostracod assemblage from one site in the circalittoral zone of Pontine Archipelago, in the central-eastern Tyrrhenian Sea, is presented. The new Specific Population Stage Index (SPS) is proposed, built upon the measurements of all growth stages in the assemblage. The population structure using the new SPS Index on three different grain sizes is tested against a list of putative *in situ* and transported ostracod specimens. The analysis on the small grain size (maximum heigth >63 μm) proved the most effective in describing the putative life ostracod assemblage, whereas in the largest grain size (maximum height >180 μm) the young instars of the smaller species are under-represented. This includes species generally under-represented in the fossil record of the Mediterranean, probably due to sample processing bias and not to the rarity of the species itself. Assessing the autochthoneity of modern/fossil assemblages has great potential for acquiring baseline information on ecosystems before the onset of human activities, making this an extremely powerful approach essential to evaluating anthropogenic impacts. This approach seeks to identify the *in situ* life assemblages within an ostracod population to ensure that paleoenvironmental interpretations are not biased by transported allochthonous elements.

1. Introduction

During the last two decades, conservation paleobiology has become an important discipline that unites the goal of applying geological and historical records to inform the conservation-restoration of biodiversity and ecosystem services (Dillon et al., 2022). For benthic fauna, differences between the composition of a time-averaged death assemblage and the local living community have been typically attributed to natural postmortem processes (Kidwell, 2007). Concerning benthic microfauna, one of the main issues is the conflation of fossil and modern assemblages. The modern assemblages refer to accumulation occurring at present (Gibbard and Head, 2020) and can be mixed with fossil assemblages through transport and diagenetic processes challenging distribution patterns interpretation.

Ostracods exhibit discontinuous growth by moulting their calcified exoskeleton, a process that involves the secretion of a new bivalved carapace during the ecdysis. As like for all arthropods, moulting is necessary to replace the previous, smaller, inflexible carapace. The two calcitic valves, discarded during moulting, may become a biotic component of the bottom sediment, forming part of a death assemblage. The majority of living benthic ostracod species reach maturity through eight juvenile stages, consequently each individual can be potentially represented in the thanatocoenosis by sixteen juvenile and two adult valves (Boomer et al., 2003). The occurrence in modern and fossil assemblages of young and adult instars, and their proportion, depends on taphonomic processes, including postmortem transport and mechanical destruction or chemical dissolution of the thinner and more delicate shells. In addition, the processing of the samples tends to remove the smallest size-fraction of the sediments, resulting in the loss of early in-

* Corresponding author.
E-mail address: roberta.parisi@igag.cnr.it (R. Parisi).

https://doi.org/10.1016/j.revmic.2023.100755
Received 13 October 2023; Received in revised form 1 December 2023; Accepted 3 December 2023

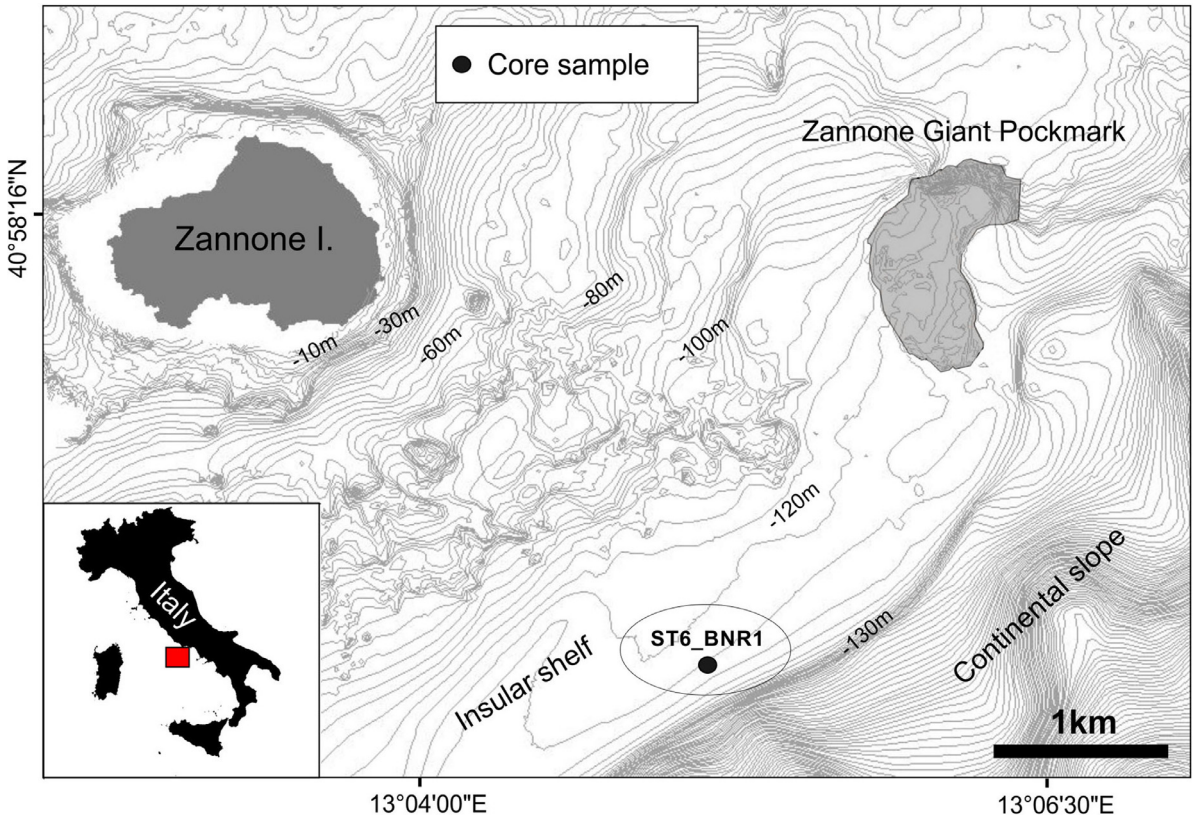

Fig. 1. Bathymetric map of the area and core location.

Table 1
Length ranges of different development stages (in mm); A corresponds to adult stage, A-n corresponds to different development stages.

	A	A-1	A-2	A-3	A-4	A-5	A-6	A-7	A-8
Neonesidea mediterranea	1.13–1.32	0.97–1.11	0.88–0.94	0.84	0.64–0.73	0.50–0.59	0.38–0.45	0.28–0.36	0.22–0.27
Bosquetina tarentina	1.15–1.23	0.88–0.97	0.82	0.70–0.72	0.63				
Neonesidea formosa				0.47–0.53	0.44	0.37–0.40	0.29–0.32		
Urocythereis ilariae	0.98	0.77	0.56–0.59	0.46–0.47	0.35	0.27			
Aurila convexa + interpretis + speyeri	0.88–1.00	0.72–0.83	0.57–0.69	0.43–0.53	0.35–0.41	0.31–0.33		0.23–0.24	
Carinocythereis carinata + whitei	0.90–0.99	0.74–0.78	0.55–0.62	0.43–0.47	0.37				
Pontocypris acuminata	0.77	0.69–0.70		0.49	0.39–0.41	0.29–0.34			
Cytherella vulgatella	0.71–0.75	0.59–0.69	0.50–0.55	0.41–0.45			0.23		
Paracytheridea triquetra	0.69–0.76	0.56–0.62	0.51–0.55	0.41–0.49	0.38	0.28–0.30	0.23–0.25		
Loxoconcha ovulata	0.66–0.80	0.50–0.55	0.46–0.49	0.40–0.44	0.32–0.33	0.23–0.26			
Monoceratina oblita	0.67–0.74	0.61	0.47	0.43					
Loxoconcha affinis	0.58–0.69	0.48–0.56	0.46	0.35–0.39		0.23–0.25			
Xestoleberis plana		0.47–0.50	0.45	0.37–0.40	0.27–0.31	0.24–0.25	0.20–0.22		
Xestoleberis dispar + aff. *perula*	0.45–0.64	0.39–0.44	0.34–0.38	0.29–0.33	0.26–0.28	0.22–0.25	0.18–0.21	0.16–0.17	
Argilloecia robusta	0.50–0.56	0.44	0.38	0.28–0.30					
Callistocythere crispata + flavidofusca	0.49–0.56	0.43–0.47	0.38–0.42	0.34–0.37	0.30–0.31	0.25	0.20		
Xestoleberis communis	0.47–0.55	0.43–0.46	0.37–0.41	0.29–0.33	0.24–0.28	0.20–0.23	0.15–0.19	0.14	
Dopseucythere mediterranea	0.48–0.53	0.43–0.47			0.25				
Semicytherura paradoxa	0.44–0.58	0.39		0.28					
Semicytherura acuticostata	0.40–0.52		0.33						
Semicytherura aenariensis + heinzei	0.40–0.52		0.30–0.31	0.24					
Buntonia sublatissima	0.46–0.50	0.42							
Eucythere curta	0.43–0.52	0.34–0.37		0.23					
Callistocythere praecincta	0.41–0.47	0.36		0.23–0.26					
Microxestoleberis xenomys	0.40–0.41	0.34–0.35	0.27–0.30	0.23–0.24	0.19–0.21	0.14–0.16			
Microcytherura angulosa	0.40–0.51	0.34–0.39	0.26–0.30	0.20–0.24	0.17–0.18				
Semicytherura alifera	0.38–0.49	0.35	0.32	0.25–0.28					
Semicytherura dispar	0.38–0.44	0.31							
Hemicytherura defiorei + videns	0.31–0.40	0.27–0.30	0.22	0.19	0.15				
Kangarina abyssicola	0.30–0.38	0.27–0.29	0.22–0.24	0.2					
Semicytherura rara	0.30–0.37	0.27–0.28							
Microcythere inflexa	0.26–0.34	0.20–0.25	0.16–0.18						
Cluthia keiji	0.31–0.32	0.27	0.23–0.24	0.20–0.22					
Microcythere depressa	0.24–0.31	0.20–0.23							
Microcythere hians	0.23–0.31	0.20–0.22	0.16–0.18						

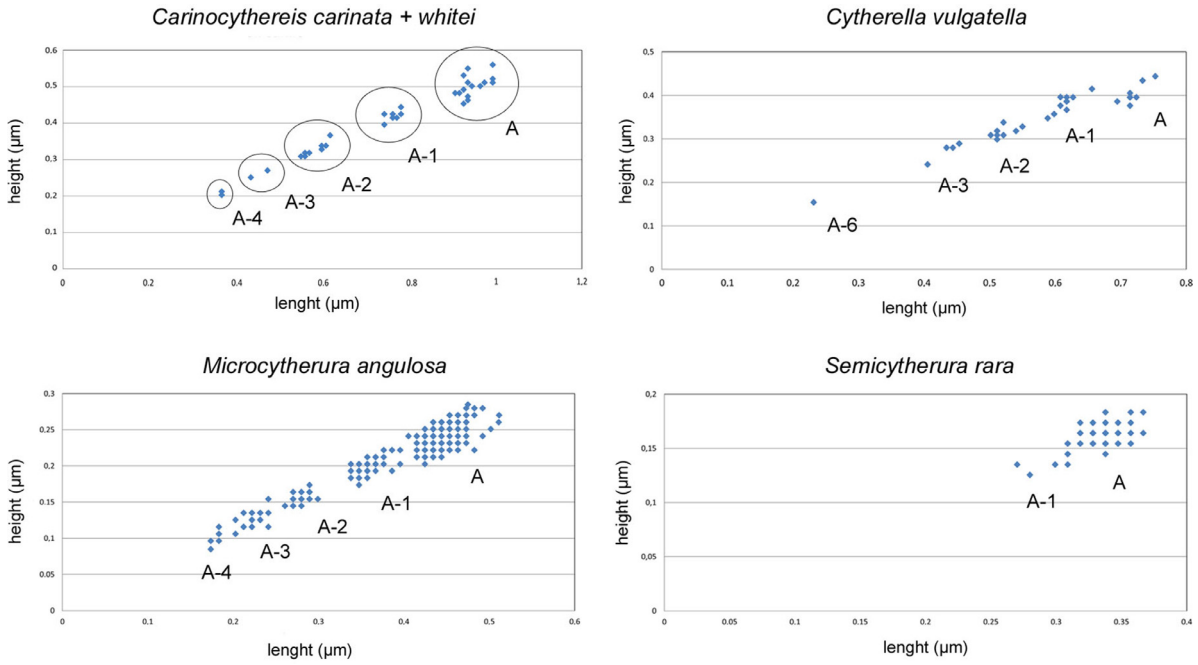

Fig. 2. Length-height diagrams (De Deckker, 2002) of different development stages for specimens of four species (*Carinocythereis crispata + flavidofusca, Microcytherura angulosa, Cytherella vulgatella, Semicytherura rara*). A corresponds to adult stage, A-n corresponds to different development stages.

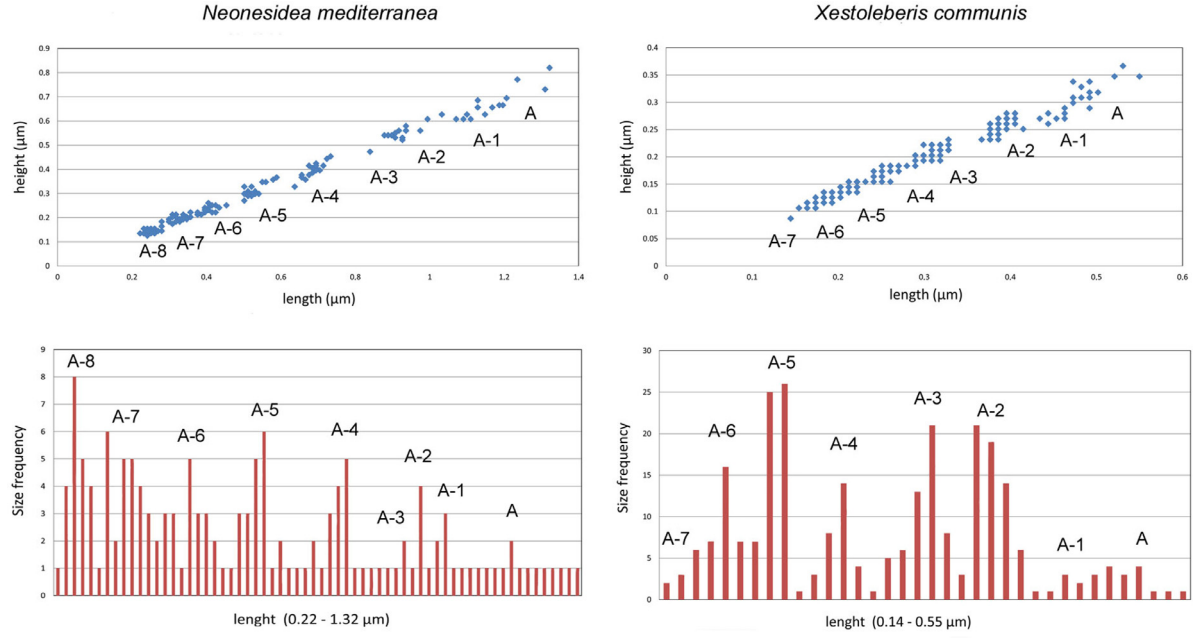

Fig. 3. Comparison between Population Age Structure length-height diagrams (De Deckker, 2002) and size frequency distribution (Danielopol et al., 2008) for the two species *Neonesidea mediterranea* and *Xestoleberis communis*.

Table 2
Total number of valves for different grain sizes and number of valves used for population age structure and statistical analyses.

	63µ	125µ	180µ
Total valves	2571	2224	1647
Structure histograms	2440	2099	1549
Statistical analyses	2259	1861	1353

stars of large-sized species and of almost all the juveniles of small-sized taxa (Brouwers, 1988).

The quantitative estimation of the population age structure is an appropriate tool for assessing the influence of some environmental parameters on dead assemblages and for determining the autochthoneity or allochthoneity of the species that make up the thanatocoenosis. Whatley (1983, 1988), van Harten (1986) and Boomer et al. (2003) proposed some type-histograms displaying population age structures characteris-

Table 3
A:J ratio for the three grain sizes for all analyzed subsamples.

Ratio A/j	B_N 0–1	B_N 1–2	B_N 2–3	B_N 3–4	B_N 4–5	B_N 5–6	B_N 6–7	B_N 7–8	B_N 8–9
h > 63 μm; tot valves	0.98	0.95	0.84	0.87	1.29	1.06	1.13	0.78	1.04
h > 63 μm; > 10 measurable valves	1.02	0.96	0.83	0.92	1.29	1.04	1.17	0.80	1.03
h > 125 μm; tot valves	1.00	0.94	0.88	0.91	1.22	1.11	1.05	0.74	0.97
h > 125 μm; > 10 measurable valves	1.04	0.95	0.86	0.97	1.21	1.08	1.07	0.75	0.95
h > 180 μm; tot valves	1.02	0.89	1.11	1.08	1.31	1.39	1.70	1.06	1.25
h > 180 μm; > 10 measurable valves	1.03	0.90	1.09	1.12	1.33	1.38	1.79	1.08	1.21

Table 4
SPS range and mean value for species with at least 10 measurable valves for *h* >63 μm.

species/SPS	Range	Mean
Argilloecia robusta	0 - 6.00	2.69
Aurila convexa + interpretis + speyeri	5.43 - 6.91	6.04
Bosquetina tarentina	0 - 7.87	5.78
Buntonia sublatissima	0 - 7.00	3.81
Callistocythere crispata + flavidofusca	4.50 - 7.57	6.16
Callistocythere praecincta	4.50 - 7.55	5.77
Carinocythereis carinata + whitei	4.50 - 7.30	6.02
Cluthia keiji	0 - 6.75	4.69
Cytherella vulgatella	0 - 7.44	5.22
Dopseucythere mediterranea	0 - 7.33	3.79
Eucythere curta	0 - 7.88	5.24
Hemicytherura defiorei + videns	6.00 - 8.52	7.70
Kangarina abyssicola	0 - 6.57	3.03
Loxoconcha affinis	0 - 7.38	4.26
Loxoconcha ovulata	5.00 - 7.17	6.13
Microcythere depressa	4.50 - 8.31	7.36
Microcythere hians	4.50 - 8.68	7.44
Microcythere inflexa	7.00 - 8.29	7.62
Microcytherura angulosa	8.05 - 8.35	8.22
Microxestoleberis xenomys	0 - 6.00	4.46
Monoceratina oblita	0 - 6.25	3.88
Neonesidea formosa	0 - 4.14	1.95
Neonesidea mediterranea	2.15 - 5.21	3.58
Paracytheridea triquetra	3.00 - 6.69	5.88
Pontocypris acuminata	0 - 4.80	2.38
Semicytherura acuticostata	6.00 - 8.36	7.57
Semicytherura aenariensis + heinzei	0 - 7.71	4.66
Semicytherura alifera	6.75 - 8.54	7.97
Semicytherura dispar	0–7.50	5.31
Semicytherura paradoxa	0 - 7.00	4.50
Semicytherura rara	7.71 - 8.55	8.29
Urocythereis ilariae	0 - 6.00	1.53
Xestoleberis communis	4.57 - 6.24	5.30
Xestoleberis dispar	4.53 - 6.50	5.39
Xestoleberis plana + aff. *perula*	0 - 5.30	3.67

Table 5
SPS range and mean value for species with at least 10 measurable valves for *h* >125 μm.

species/SPS	Range	Mean
Argilloecia robusta	0 - 6.00	2.69
Aurila convexa + interpretis + speyeri	5.43 - 6.91	6.04
Bosquetina tarentina	0 - 7.87	5.78
Buntonia sublatissima	0 - 7.00	3.81
Callistocythere crispata + flavidofusca	4.50 - 7.57	6.16
Callistocythere praecincta	4.50 - 7.55	5.77
Carinocythereis carinata + whitei	4.50 - 7.30	6.02
Cluthia keiji	0 - 6.75	4.69
Cytherella vulgatella	0 - 7.44	5.22
Dopseucythere mediterranea	0 - 7.33	3.79
Eucythere curta	0 - 7.88	5.24
Hemicytherura defiorei + videns	6.00 - 8.52	7.73
Kangarina abyssicola	0 - 6.67	3.04
Loxoconcha affinis	0 - 7.38	4.26
Loxoconcha ovulata	5.00 - 7.17	6.13
Microcythere depressa	0 - 6.75	1.25
Microcythere hians	0 - 6.00	1.83
Microcythere inflexa	0 - 8.18	5.47
Microcytherura angulosa	8.18 - 8.53	8.29
Microxestoleberis xenomys	0 - 6.00	4.10
Monoceratina oblita	0 - 6.25	3.88
Neonesidea formosa	0 - 4.14	1.95
Neonesidea mediterranea	2.79 - 5.21	3.72
Paracytheridea triquetra	3.00 - 6.80	6.11
Pontocypris acuminata	0 - 4.80	2.38
Semicytherura acuticostata	6.00 - 8.36	7.57
Semicytherura aenariensis + heinzei	0 - 7.71	4.66
Semicytherura alifera	6.75 - 8.55	7.98
Semicytherura dispar	0–7.50	5.31
Semicytherura paradoxa	0 - 7.00	4.50
Semicytherura rara	7.71 - 8.55	8.29
Urocythereis ilariae	0 - 6.00	1.53
Xestoleberis communis	4.76 - 6.48	5.47
Xestoleberis dispar	5.10 - 6.50	5.75
Xestoleberis plana + aff. *perula*	0 - 5.30	3.74

tic of autochthonous, allochthonous and mixed (*sensu* Fagerstrom, 1964) assemblages formed in various environments and paleoenvironments. The population age structure is infrequently used to test autochthoneity of both fossil and modern ostracods, possibly because of the time-consuming nature of microscope measurements required for this analysis (do Carmo et al., 1999; Fontana and Ballent, 2005).

A simpler mode of detecting if an ostracod assemblage is transported or is *in situ* was applied by Brouwers (1988, and literature therein) using the adult to juvenile ratio. This method does not require shell measurement to establish the developmental stage of all valves, but only to assess if they belonged to adult or young instars.

Subsequent investigations have considered assemblages and/or single species in shallow marine (Ruiz et al., 2003) and lacustrine (Zhai et al., 2013, 2015; Mao et al., 2021) environments and their relationship with grain size, water depth, hydrological conditions, and downslope contamination. In lacustrine environments, it is assumed that a death assemblage integrates, through accumulation and time averaging, several generations over time and incorporates species which are rare or absent in life assemblages, and accumulates species assemblages corresponding to a larger range of environmental fluctuations related to grain size, water depth, hydrological conditions, and downslope contamination (Zhai et al., 2013, 2015; Mao et al., 2021; Hoehle and Wrozyna, 2022). In marine environments, the population structure of halocyprid ostracods at high latitudes has been seldom studied (Blachowiak-Samolyk and Angel, 2007) as well as the Mediterranean benthic ostracod total and living assemblages (Ruiz et al., 1997, 2003).

The aim of the present study is to test whether methods based on population age structure are appropriate in determining autochthonous and allochthonous components of live/dead ostracod assemblages.

2. Material and methods

We analysed nine subsamples collected from one site in the circalittoral zone of Pontine Archipelago, in the central-eastern Tyrrhenian Sea, which yielded rich and well-preserved dead ostracod faunas previously investigated by Aiello et al. (2022) in order to assess the influence of carbon dioxide emissions on calcareous meiobenthic assem-

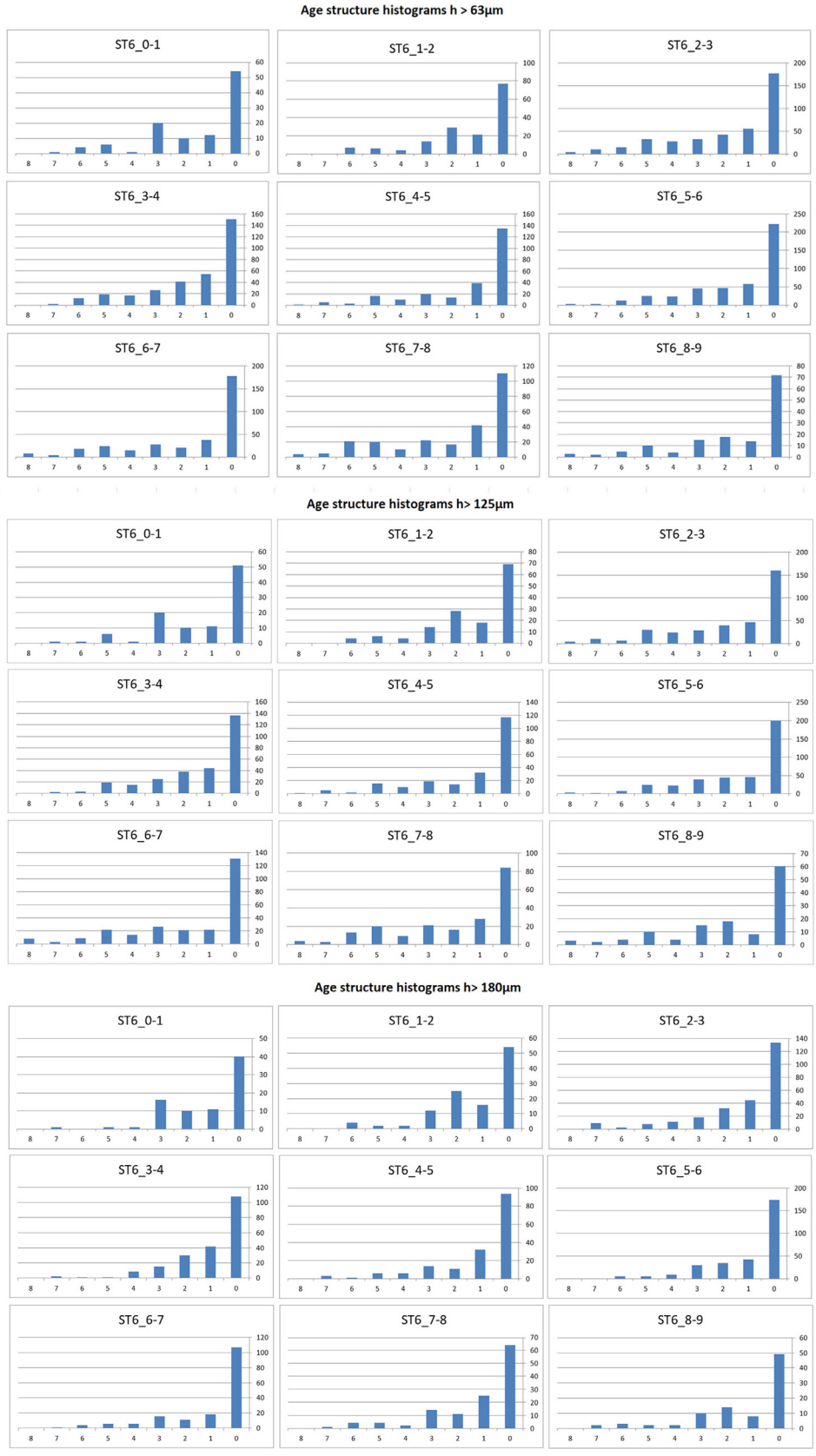

Fig. 4. Assemblage Population Age Structure histograms calculated for h >63 µm, h >125 µm and h >180 µm; 0 corresponds to adults and 1–8 to development stages.

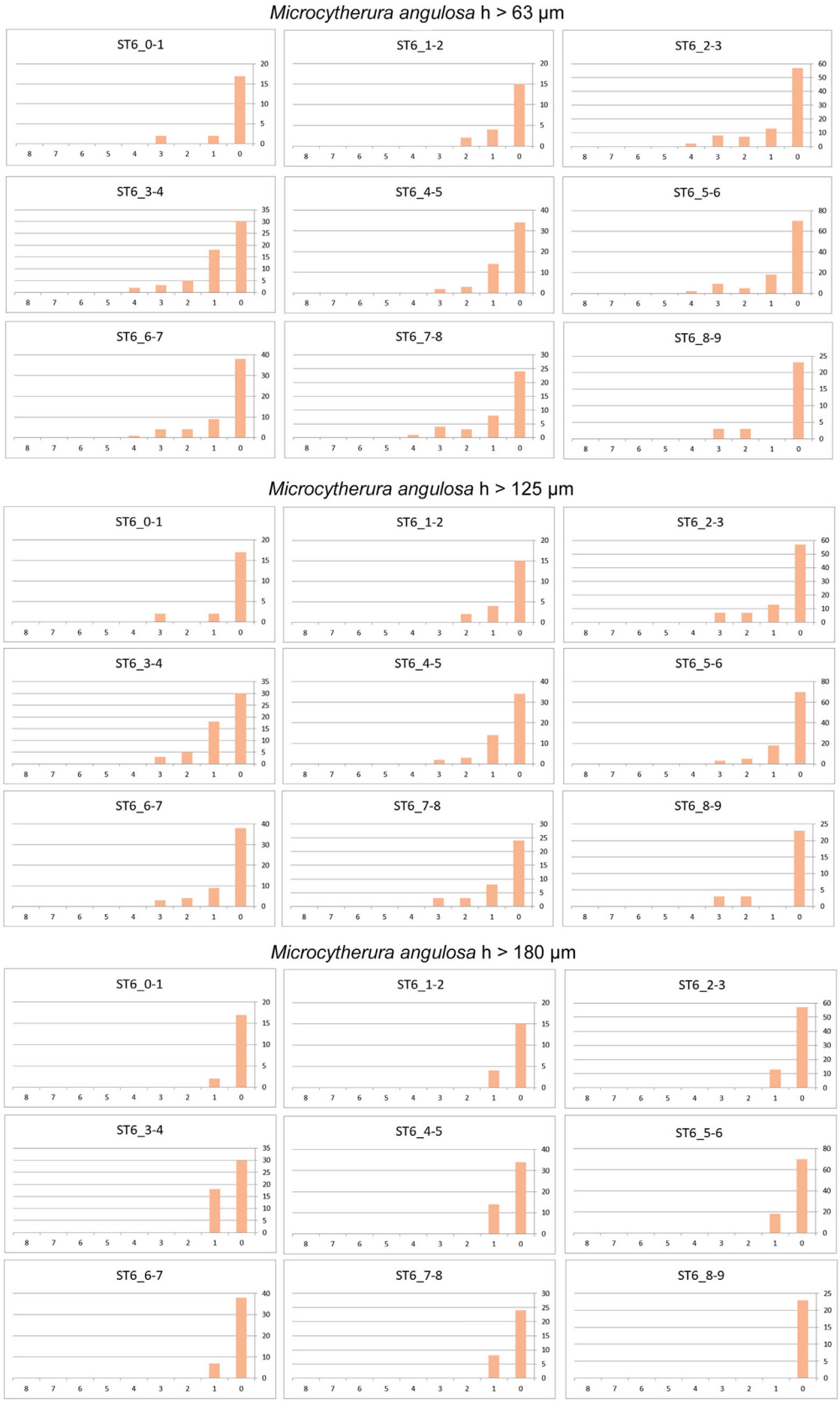

Fig. 5. *Microcytherura angulosa* specific Population Age Structure histograms for *h* >63 µm, *h* >125 µm and *h* >180 µm; 0 corresponds to adults and 1–8 to development stages.

Fig. 6. *Neonesidea mediterranea* specific Population Age Structure histograms. The histograms for *h* >63 µm are the same as *h* >125 µm, whereas the histogram for *h* >180 µm is different; 0 corresponds to adults and 1–8 to development stages.

blages around the hydrothermal vent system of the Zannone Giant Pockmark (Ingrassia et al., 2015).

A short core (ST6_BNR1, 13°05′12.9495″ E, 40°56′56.8619″ N) sampled at 127 m bsl during the research cruise "Bolle 2014" on the eastern Zannone insular shelf by means of a 30 L Van Veen grab, was sliced in one cm layers to a depth of 9 cm, obtaining nine subsamples (Di Bella et al., 2016) (Fig. 1, modified from Aiello et al., 2022). Quantitative analyses of the ostracod assemblages (Aiello et al., 2022) were performed on sediment grain size >63 µm. Discrimination between live and dead specimens was not attempted. In fact, although all sediment samples were stained and preserved in a solution of 2 g/l of Rose Bengal and ethanol for 15 days before sieving (Di Bella et al., 2016), this method is not suitable for a clear discrimination between 'living' and 'dead' ostracod assemblages (Danielopol et al., 2002; Horne et al., 2021).

In the present study we have critically reviewed the distribution data reported in classic and modern literature on Mediterranean ostracods (Müller, 1894; Barbeito-Gonzales, 1971; Uffenorde, 1972; Bonaduce et al., 1976, 1977; Breman, 1976; Aiello and Barra, 2010; Aiello et al., 2006, 2018, 2021; Balassone et al., 2016; Mangoni et al., 2016) to identify the allochthoneity or autochthoneity of dominant and

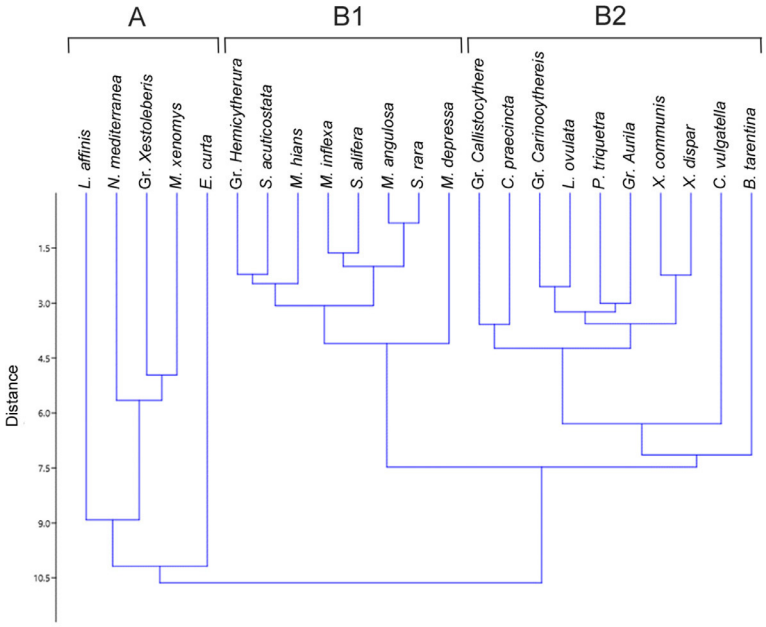

Fig. 7. Dendrogram resulting from cluster analysis (paired group algorithm and Euclidean distance) for valves with *h* >63 μm using the SPS index (*Gr. Aurila* = *A. convexa* + *interpretis* + *speyeri*; Gr. *Hemicytherura* = *H. defiorei* + *videns*; Gr. *Callistocythere* = *C. crispata* + *flavidofusca*; Gr. *Carinocythereis* = *C. carinata* + *whitei;* Gr. *Xestoleberis* = *X. dispar* + aff. *perula*).

Table 6
SPS range and mean value for species with at least 10 measurable valves for *h* >180 μm.

species/SPS	Range	Mean
Argilloecia robusta	0 - 6.00	2.69
Aurila convexa + interpretis + speyeri	5.50 - 6.91	6.09
Bosquetina tarentina	0 - 7.87	5.78
Buntonia sublatissima	0 - 7.00	3.81
Callistocythere crispata + flavidofusca	4.50 - 7.57	6.30
Callistocythere praecincta	4.50 - 7.89	5.85
Carinocythereis carinata + whitei	4.50 - 7.30	6.02
Cluthia keiji	0 - 6.00	2.67
Cytherella vulgatella	0 - 7.44	5.28
Dopseucythere mediterranea	0 - 7.33	3.81
Eucythere curta	0 - 7.88	5.19
Hemicytherura defiorei + videns	6.00 - 8.36	6.50
Kangarina abyssicola	0 - 6.00	1.67
Loxoconcha affinis	0 - 7.38	4.40
Loxoconcha ovulata	5.00 - 7.17	6.20
Microcytherura angulosa	8.35 - 8.70	8.55
Microxestoleberis xenomys	0 - 5.67	2.61
Monoceratina oblita	0 - 6.25	3.88
Neonesidea formosa	0 - 4.14	1.95
Neonesidea mediterranea	3.25 - 5.21	4.23
Paracytheridea triquetra	3.00 - 7.38	6.23
Pontocypris acuminata	0 - 5.00	1.86
Semicytherura acuticostata	6.00 - 8.31	7.58
Semicytherura aenariensis + heinzei	0 - 7.71	4.61
Semicytherura alifera	6.75 - 8.63	8.04
Semicytherura dispar	0–7.50	4.67
Semicytherura paradoxa	0 - 7.20	4.52
Semicytherura rara	7.71 - 8.55	1.67
Urocythereis ilariae	0 - 6.25	1.56
Xestoleberis communis	6.00 - 6.94	6.36
Xestoleberis dispar	5.60 - 7.55	6.70
Xestoleberis plana + aff. *perula*	0 - 5.75	3.08

characteristic species based on their autoecological characteristics and distribution.

All the 3842 valves studied by Aiello et al. (2022) have been observed, measured and divided in size classes depending on their maximum of height (63 μm, 125 μm, 180 μm). The damaged specimens, mostly represented by delicate taxa such as *Neonesidea*, were excluded and the length/height of the 2571 valves with intact shell margins have been measured (Appendix 1).

2.1. The Adult:Juveniles ratio

For the calculation of the A:J ratio (Adult:Juveniles ratio) of the nine subsamples, all the 2571 measurable valves have been considered, whereas for the definition of the population age structure only the species occurring with at least 10 measurable valves have been considered. The assignment of the valves to growth stages required the measurements of the maximal height (h) and length (l) for each specimen and the construction of Table 1, in which all the length measurements are grouped in ranges, corresponding to development stages. In most cases, the A-5/A-8 stages are lacking (Fig. 2; *Carinocythereis carinata* + *whitei* and *Microcytherura angulosa*). In some cases, intermediate stages are absent (Fig. 2; *Cytherella vulgatella*), while in other cases only adults and A-1 stages occur (Fig. 2; *Semicytherura rara*). *Neonesidea mediterranea* is the only species in which all the stages (A/A-8) occur, in *Xestoleberis communis* only A-8 stage is lacking (Fig. 3). Adult specimens of *Neonesidea formosa* do not occur. Adult valves and penultimate instars of *Buntonia sublatissima, Microcythere depressa* and *Semicytherura dispar* and *Semicytherura rara* are present, whereas A-2/A-8 stages lack (Table 1).Consequently, 2440 valves have been used to build the population age structure histograms (further details in Table 2).

To compare the results obtained using different mesh sizes, A:J ratio has been calculated in three ways (Table 3): a - considering all the valves (*h* >63 μm); b - using the valves with *h* >125 μm following Boomer et al. (2003); c - using the valves with *h* >180 μm following the Brouwers (1988) procedure.

2.2. The population age structure and the new SPS index

The definition of population age structure was obtained comparing length-height diagrams (*e.g.,* De Deckker, 2002) and size frequency distribution (*e.g.,* Danielopol et al., 2008) for each species (Figs. 2-3). All the valves have been assigned to a growth stage (Table 1), and a population age structure diagram for each of the nine subsamples has been developed.

Considering previous studies and how to distinguish between autochthonous and allochthonous assemblages, a new index is pro-

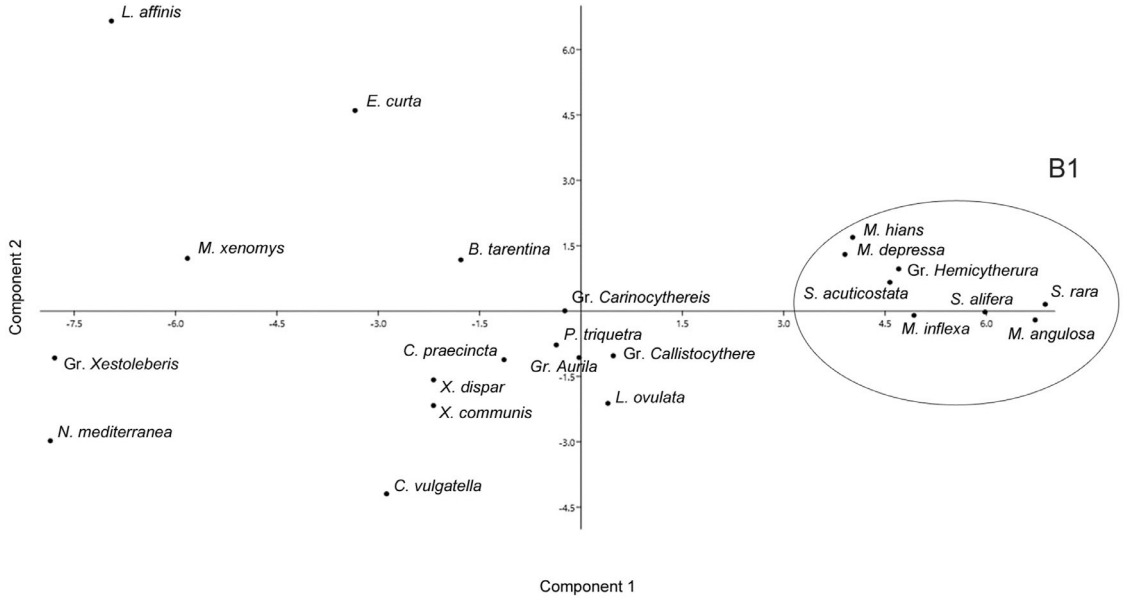

Fig. 8. Principal Cluster Analysis (PCA) performed on valves with *h* >63 μm using the SPS index. The circle groups autochthonous species characterized by high SPS values (*Gr. Aurila* = *A. convexa* + *interpretis* + *speyeri*; Gr. *Hemicytherura* = *H. defiorei* + *videns*; Gr. *Callistocythere* = *C. crispata* + *flavidofusca*; Gr. *Carinocythereis* = *C. carinata* + *whitei;* Gr. *Xestoleberis* = *X. dispar* + aff. *perula*).

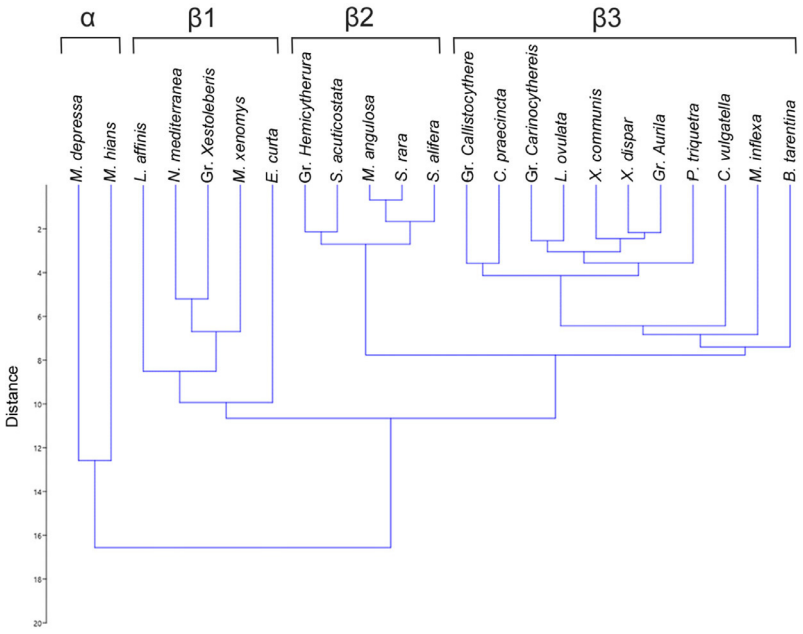

Fig. 9. Dendrogram resulting from cluster analysis (paired group algorithm and Euclidean distance) for valves with *h* >125 μm using the SPS index (*Gr. Aurila* = *A. convexa* + *interpretis* + *speyeri*; Gr. *Hemicytherura* = *H. defiorei* + *videns*; Gr. *Callistocythere* = *C. crispata* + *flavidofusca*; Gr. *Carinocythereis* = *C. carinata* + *whitei;* Gr. *Xestoleberis* = *X. dispar* + aff. *perula*).

posed modifying the Mean Population Index (MPS) presented by Marin (1987) for copepod populations, subsequently modified by Kock (1992) for epipelagic ostracods, and by Zhai et al. (2015) and Mao et al. (2021) for benthic freshwater ostracods.

We define the SPS = Specific Population Stage Index as follows:

$$SPS = \left[\left(I_{A-8}\times 1\right)+\left(I_{A-7}\times 2\right)+\left(I_{A-6}\times 3\right)+\left(I_{A-5}\times 4\right)+\left(I_{A-4}\times 5\right)+\left(I_{A-3}\times 6\right)+\left(I_{A-2}\times 7\right)+\left(I_{A-1}\times 8\right)+\left(I_{A}\times 9\right)\right] / \left[1+\left(I_{A-8}+I_{A-7}+I_{A-6}+I_{A-5}+I_{A-4}+I_{A-3}+I_{A-2}+I_{A-1}+I_{A}\right)\right]$$

where I_A is the number of adult instars of the considered species in the studied sample, I_{A-1} the number of penultimate instars, etc. It must be noted that SPS values range from 0 to 9 (when the species is not present the numerator is equal to zero and SPS = 0; when $I_A \rightarrow \infty$, SPS → 9).

For each of the nine subsamples, the mean value for species with at least 10 measurable valves has been calculated (*h* >63 μm: 2440 valves; *h* >125 μm: 2099 valves; *h* >180 μm: 1549 valves) (Tables 4-6).

2.3. Statistical analyses

R-mode cluster analysis with Euclidean similarity index (algorithm paired group) and Principal Component Analysis were carried out using the freeware PAST version 4.06b (Hammer et al., 2001) on the SPS index values of the species with more than 20 measurable valves. Consequently, 2259 valves have been used for statistical analyses.

3. Results

The comparison with the distribution data reported for the Mediterranean Sea suggested the discrimination of three groups. Group 1

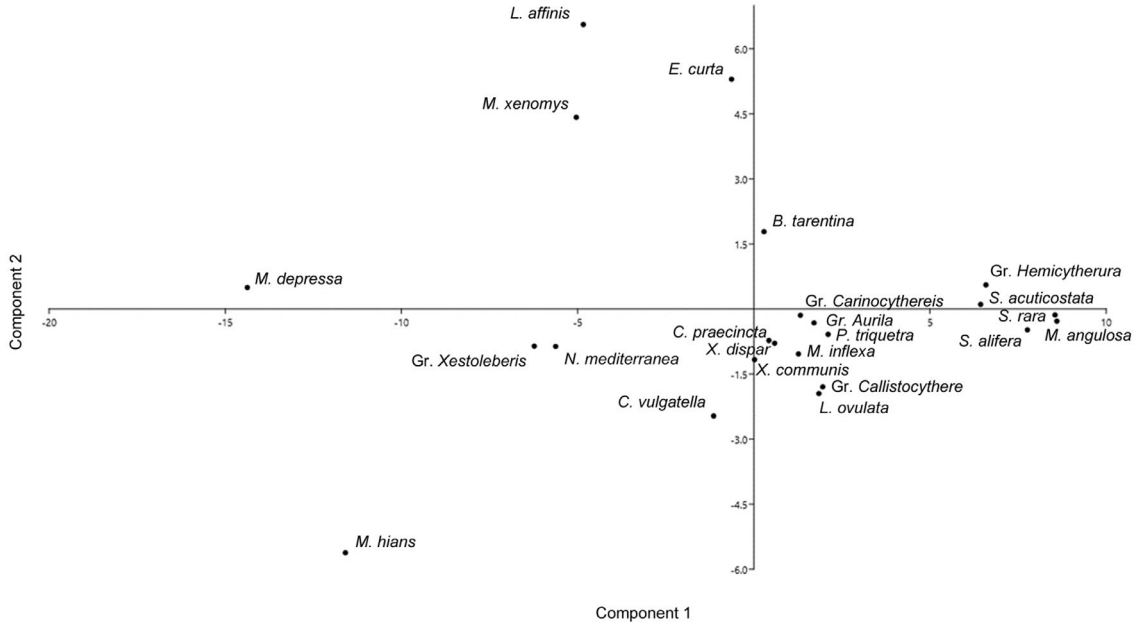

Fig. 10. Principal Cluster Analysis (PCA) performed on valves with *h* >125 μm using the SPS index (*Gr. Aurila* = *A. convexa* + *interpretis* + *speyeri*; Gr. *Hemicytherura* = *H. defiorei* + *videns*; Gr. *Callistocythere* = *C. crispata* + *flavidofusca*; Gr. *Carinocythereis* = *C. carinata* + *whitei;* Gr. *Xestoleberis* = *X. dispar* + aff. *perula*).

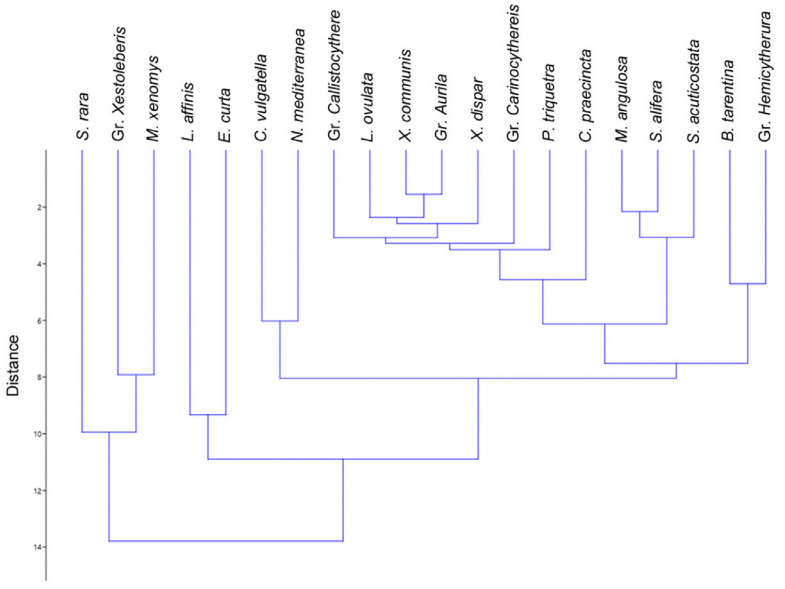

Fig. 11. Dendrogram resulting from cluster analysis (paired group algorithm and Euclidean distance) for valves with *h* >180 μm using the SPS (*Gr. Aurila* = *A. convexa* + *interpretis* + *speyeri*; Gr. *Hemicytherura* = *H. defiorei* + *videns*; Gr. *Callistocythere* = *C. crispata* + *flavidofusca*; Gr. *Carinocythereis* = *C. carinata* + *whitei;* Gr. *Xestoleberis* = *X. dispar* + aff. *perula*).

includes putative autochthonous species; Group 2 consists of displaced species; Group 3 is formed by problematic species, *i.e.,* possibly occurring with both autochthonous and displaced specimens (Table 7).

The A:J ratio (Table 3) calculated for the 9 subsamples shows the following ranges: from 0.78 to 1.29 in the analysis considering all the measurable valves (*h* >63 μm); from 0.80 to 1.29 using the taxa with >10 measurable valves (*h* >63 μm); from 0.74 to 1.22 considering all the measurable valves (*h* >125 μm); from 0.75 to 1.21 using the taxa with >10 measurable valves (*h* >125 μm); from 0.89 to 1.70 when analysing all the individuals with *h* >180 μm; from 0.90 to 1.79 in the analysis considering the taxa with >10 measurable valves.

The number of valves for each stage varies depending on the mesh choice (Tables 8-10). For example, in *Microcytherura angulosa*, which is the most abundant species, A/A-4 stages occur. It is a relatively small species, and consequently A-5/A-8 stages are not present. The total number of valves is, respectively of 469 (*h* >63 μm), 452 (*h* >125 μm) and 392 (*h* >180 μm). In all three cases, the number of adult valves equals to 308.

In general, the assemblage population age structure histograms display some differences when calculated for *h* >63 μm, *h* >125 μm and *h* >180 μm (Fig. 4): in the latter case, the young instars of the smaller species are under-represented. Similarly, the specific population age structure histograms show slight variations for *h* >63 μm, *h* >125 μm and *h* >180 μm (Figs. 5, 6).

The SPS, which is equal to zero when the species is not present in the assemblage, has different values when calculated for *h* >63 μm, *h* >125 μm and *h* >180 μm.

For *h* >63 μm, *Microcythere hians* has the highest value, SPS = 8.68 (mean 7.44), in sample B_N 6-7 (Table 4). *Semicytherura rara* and *Micro-*

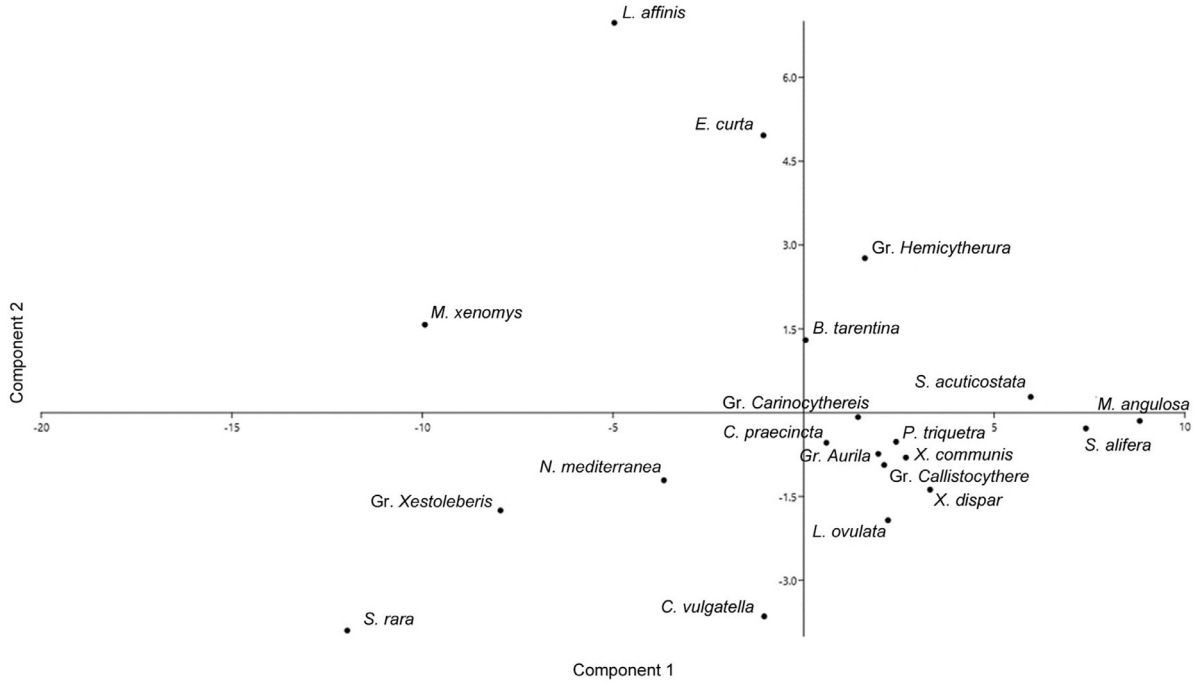

Fig. 12. Principal Cluster Analysis (PCA) performed on valves with *h* >180 μm using the SPS index (*Gr. Aurila* = *A. convexa* + *interpretis* + *speyeri*; Gr. *Hemicytherura* = *H. defiorei* + *videns*; Gr. *Callistocythere* = *C. crispata* + *flavidofusca*; Gr. *Carinocythereis* = *C. carinata* + *whitei;* Gr. *Xestoleberis* = *X. dispar* + aff. *perula*).

Table 7
List of species from literature data divided in groups depending on their putative autochthoneity/allochthoneity.

Group 1	Group 2	Group 3
autochthonous species	displaced species	problematic species
Argilloecia robusta	*Neonesidea formosa*	*Aurila convexa* + *interpretis* + *speyeri*
Bosquetina tarentina	*Neonesidea mediterranea*	*Carinocythereis carinata* + *whitei*
Buntonia sublatissima	*Urocythereis ilariae*	*Loxoconcha affinis*
Callistocythere crispata + *flavidofusca*		*Loxoconcha ovulata*
Callistocythere praecincta		*Microxestoleberis xenomys*
Cytherella vulgatella		*Paracytheridea triquetra*
Cluthia keiji		*Pontocypris acuminata*
Dopseucythere mediterranea		*Semicytherura paradoxa*
Eucythere curta		*Xestoleberis communis*
Hemicytherura defiorei + *videns*		*Xestoleberis dispar*
Kangarina abyssicola		*Xestoleberis plana* + aff. *perula*
Microcytherura angulosa		
Monoceratina oblita		
Semicytherura acuticostata		
Semicytherura aenariensis + *heinzei*		
Semicytherura alifera		
Semicytherura dispar		
Semicytherura rara		

cytherura angulosa display high SPS mean (SPSm) values, respectively equal to 8.29 and 8.22. *Neonesidea mediterranea* shows the minimum of SPS mean value (SPSm = 3.58).

For *h* >125 μm (Table 5), in sample B_N 2–3 both *Semicytherura alifera* and *Semicytherura rara* show maximal SPS (= 8.55). Both *Semicytherura rara* and *Microcytherura angulosa* have maximum of SPSm value equal to 8.29. Very low SPSm pertain to *Microcythere depressa* (SPSm = 1.25) and *Microcythere hians* (SPSm = 1.83).

For *h* >180 μm (Table 6), maximum of SPS is displayed by *Microcytherura angulosa* (SPS = 8.70) in the sample B_N 5-6. This species has the highest SPSm (8.55), followed by *Semicytherura alifera* (SPSm = 8.04). The lowest SPSm is 1.56 (in *Urocythereis ilariae*); we note the disappearance of *Microcythere depressa, hians* and *inflexa*.

The species of the Group 1 generally show both low and high values of SPSm; in the Group 2, SPSm is low-very low and in the Group 3, middle-low values of SPSm occur.

3.1. Statistical analyses

Cluster analysis using paired group algorithm and Euclidean distance, was performed on all size groups.

The dendrogram resulting from cluster analysis of valves with *h* >63 μm (Fig. 7) reveals two clusters, A and B, the cluster B consisting of two subclusters, B1 and B2. The species included in the Cluster A, except *Eucythere curta* (autochthonous), are considered partly or entirely displaced (Group 2 and Group 3) as well the species forming the cluster

Table 8
Occurrence of different development stages in all the subsamples for h >63 μm.

	Development stages	Samples								
		B_N 0–1	B_N 1–2	B_N 2–3	B_N 3–4	B_N 4–5	B_N 5–6	B_N 6–7	B_N 7–8	B_N 8–9
Aurila convexa + speyeri + interpretis	A		3				3	3		
	1		1	3	4	1	5	1	4	
	2	3	5	4	3	2	5	1	2	3
	3	2	1	3	4	2	4	2	1	3
	4				1	2	3	2	1	1
	5				1			2		
	6									
	7							2		
Bosquetina tarentina	A		3	1	8	2	3		1	1
	1			7	5	2	3	1	3	1
	2									1
	3			1	1		1			1
	4			1						
Callistocythere crispata + flavidofusca	A	1	1	7	2	3	3	4	2	1
	1	1		2	1		2	3		
	2	1		3			2	1	1	
	3			1	1		2	1		2
	4				1				1	
	5				1				1	
	6								1	
Callistocythere praecincta	A	1	1	2	3	1	7	3	1	3
	1			1			1			
	2									
	3				2		2	1		
Carinocythereis carinata + whitei	A	1	1	1	4	5	1	3	1	
	1		2	1	1	2			2	1
	2		2	1	2	1			1	1
	3			1						1
	4				1	1				
Cytherella vulgatella	A		1	1	1		5			
	1	3			1	2	2	1		2
	2		1	3	4	1		1		
	3	1	1		1	2	1			
	4									
	5									
	6			1						
Hemicytherura videns + defiorei	A	2	4	7	19	9	17	9	5	6
	1			3	1				2	
	2			1						
	3			1						
	4			1						
Loxoconcha affinis	A				3	1	5	2	4	1
	1				1	2	2		2	1
	2								1	
	3						2			
	4									
	5				2					1
Loxoconcha ovulata	A	1	3	4	3	1		5		1
	1	1	2	3	1	3	1		2	1
	2			2			1			
	3	1	1	2	1	1		4		
	4				1				1	
	5					1		1		
Microcythere depressa	A	2	1	8	11	8	3	13	10	9
	1			3	2	2	1	2	2	
Microcythere hians	A	1	5	6	3	11	18	29	14	3
	1			1		1	2	1	1	1
	2		1				3			
Microcythere inflexa	A	4	3	9	7	2	5	17	6	1
	1	3	3	4	8	4	9	13	12	5
	2			2	3				1	
Microcytherura angulosa	A	17	15	57	30	34	70	38	24	23
	1	2	4	13	18	14	18	9	8	
	2		2	7	5	3	5	4	3	3
	3	2		8	3	2	9	4	4	3
	4			2	2		2	1	1	
Neonesidea mediterranea	A			3	1	1	2	1	1	1
	1		2	2	1		2			
	2	1	3		4		3	1		2
	3		2		1					
	4		2	5	3	3	5	2		
	5	1	2	7		5	3	2	1	1
	6		4	2	1	1	4	3	3	3
	7	1		10	2	5	2	1	3	2
	8			4		1	3	8	4	3

(*continued on next page*)

Table 8 (*continued*)

	Development stages	Samples								
		B_N 0–1	B_N 1–2	B_N 2–3	B_N 3–4	B_N 4–5	B_N 5–6	B_N 6–7	B_N 7–8	B_N 8–9
Paracytheridea triquetra	A	1	2	3	5	2	1	2	1	
	1	1	1	2			3	2	3	
	2	1	1	4	2	2	6	1	1	
	3	3	1	2		3	1	2		1
	4				1		1			
	5			1	1		1			
	6		1		1		1	1	1	
Semicytherura acuticostata	A	2	7	10	6	11	13	7	8	2
	1									
	2				1					
Semicytherura alifera	A	8	6	19	9	12	23	11	9	3
	1					1	1			
	2						1			
	3			1		1		2		
Semicytherura rara	A	6	11	19	16	15	16	12	13	9
	1						1	1		
Xestoleberis communis	A	3	4			1		6	1	
	1		2	2	1	1	1		1	1
	2	3	10	10	9	2	16	5	4	5
	3	10	6	6	5	1	12	4	8	1
	4	1	1	7	2	2	7	4	4	3
	5	1	3	12	8	4	7	8	11	5
	6	2	2	5	6	2	5	5	11	1
	7							1	1	
Xestoleberis dispar	A	1	2	6	3	5	4	2	1	1
	1	2		1	4	3	1	1		1
	2	1	2	3	5	3	2	1	1	2
	3		2	2	5	3	5	1	5	2
	4			4	1	2	3	1	2	
	5	4	1	6	4	3	8	5	4	2
	6	2		7	3		1	6	4	1
	7						1		1	
Xestoleberis *plana* + aff. *perula*	A									1
	1			2	2					
	2			1						
	3			1	1	3		3	1	1
	4		1	4	2		3	4		
	5			1	1	2		3		
	6				1			2		

Table 9
Occurrence of different development stages in all the subsamples for h >125 μm.

	Development stages	Samples								
		B_N 0–1	B_N 1–2	B_N 2–3	B_N 3–4	B_N 4–5	B_N 5–6	B_N 6–7	B_N 7–8	B_N 8–9
Aurila convexa + speyeri + interpretis	A		3				3	3		
	1		1	3	4	1	5	1	4	
	2	3	5	4	3	2	5	1	2	3
	3	2	1	3	4	2	4	2	1	3
	4				1	2	3	2	1	1
	5				1			2		
	6									
	7							2		
Bosquetina tarentina	A		3	1	8	2	3		1	1
	1			7	5	2	3	1	3	1
	2									1
	3			1	1		1			1
	4			1						
Callistocythere crispata + flavidofusca	A	1	1	7	2	3	3	4	2	1
	1	1		2	1		2	3		
	2	1		3			2	1	1	
	3			1	1		2	1		2
	4				1				1	
	5				1				1	
Callistocythere praecincta	A	1	1	2	3	1	7	3	1	3
	1			1			1			
	2									
	3				2		2	1		
Carinocythereis carinata + whitei	A	1	1	1	4	5	1	3	1	
	1		2	1	1	2			2	1
	2		2	1	2	1			1	1

(*continued on next page*)

Table 9 (*continued*)

	Development stages	Samples								
		B_N 0–1	B_N 1–2	B_N 2–3	B_N 3–4	B_N 4–5	B_N 5–6	B_N 6–7	B_N 7–8	B_N 8–9
	3			1						1
	4				1	1				
Cytherella vulgatella	A		1	1	1		5			
	1	3			1	2	2	1		2
	2		1	3	4	1		1		
	3	1	1		1	2	1			
	4									
	5									
	6			1						
Hemicytherura videns + defiorei	A	2	4	7	19	9	17	9	5	6
	1			3	1				2	
	2			1						
Loxoconcha affinis	A				3	1	5	2	4	1
	1				1	2	2		2	1
	2								1	
	3						2			
	4									
	5				2					1
Loxoconcha ovulata	A	1	3	4	3	1		5		1
	1	1	2	3	1	3	1		2	1
	2			2			1			
	3	1	1	2	1	1		4		
	4				1				1	
	5					1		1		
Microcythere depressa	A				3					1
Microcythere hians	A			2		1		2		
Microcythere inflexa	A	2	1	4	2	2	4	10	3	
Microcytherura angulosa	A	17	15	57	30	34	70	38	24	23
	1	2	4	13	18	14	18	9	8	
	2		2	7	5	3	5	4	3	3
	3	2		7	3	2	3	3	3	3
Neonesidea mediterranea	A			3	1	1	2	1	1	1
	1		2	2	1		2			
	2	1	3		4		3	1		2
	3		2		1					
	4		2	5	3	3	5	2		
	5	1	2	7		5	3	2	1	1
	6		4	2	1	1	4	3	3	3
	7	1		10	2	5	2	1	3	2
	8			4		1	3	8	4	3
Paracytheridea triquetra	A	1	2	3	5	2	1	2	1	
	1	1	1	2			3	2	3	
	2	1	1	4	2	2	6	1	1	
	3	3	1	2		3	1	2		1
	4				1		1			
	5			1	1		1			
Semicytherura acuticostata	A	2	7	10	6	11	13	7	8	2
	1									
	2				1					
Semicytherura alifera	A	8	6	19	9	12	23	11	9	3
	1					1	1			
	2						1			
	3					1		2		
Semicytherura rara	A	6	11	19	16	15	16	12	13	9
Xestoleberis communis	A	3	4			1		6	1	
	1		2	2	1	1	1		1	1
	2	3	10	10	9	2	16	5	4	5
	3	10	6	6	5	1	12	4	8	1
	4	1	1	7	2	2	7	4	4	3
	5	1	3	12	8	4	7	8	11	5
	6			3	2	1	2	5	8	1
Xestoleberis dispar	A	1	2	6	3	5	4	2	1	1
	1	2		1	4	3	1	1		1
	2	1	2	3	5	3	2	1	1	2
	3		2	2	5	3	5	1	5	2
	4			4	1	2	3	1	2	
	5	4	1	6	4	3	8	5	4	2
	6	1								
Xestoleberis *plana* + aff. *perula*	A									1
	1			2	2					
	2			1						
	3			1	1	3		3	1	1
	4		1	4	2		3	4		
	5			1	1	2		1		

Table 10
Occurrence of different development stages in all the subsamples for h >180 μm.

	Development stages	Samples								
		B_N 0–1	B_N 1–2	B_N 2–3	B_N 3–4	B_N 4–5	B_N 5–6	B_N 6–7	B_N 7–8	B_N 8–9
Aurila convexa + speyeri + interpretis	A		3				3	3		
	1		1	3	4	1	5	1	4	
	2	3	5	4	3	2	5	1	2	3
	3	2	1	3	4	2	4	2	1	3
	4				1	2	3	2	1	1
	5				1			2		
Bosquetina tarentina	A		3	1	8	2	3		1	1
	1			7	5	2	3	1	3	1
	2									1
	3			1	1		1			1
	4			1						
Callistocythere crispata + flavidofusca	A	1	1	7	2	3	3	4	2	1
	1	1		2	1		2	3		
	2	1		3			2	1	1	
	3			1	1		2	1		2
	4				1					
Callistocythere praecincta	A	1	1	2	3	1	7	3	1	3
	1			1			1			
	2									
	3									
Carinocythereis carinata + whitei	A	1	1	1	4	5	1	3	1	
	1		2	1	1	2			2	1
	2		2	1	2	1			1	1
	3			1						1
	4				1	1				
Cytherella vulgatella	A		1	1	1		5			
	1	3			1	2	2	1		2
	2		1	3	4	1		1		
	3	1	1		1	2	1			
Hemicytherura videns + defiorei	A		2	3	11	5	13	9	2	5
Loxoconcha affinis	A				3	1	5	2	4	1
	1				1	2	2		2	1
	2								1	
	3						2			
Loxoconcha ovulata	A	1	3	4	3	1		5		1
	1	1	2	3	1	3	1		2	1
	2			2			1			
	3	1	1	2	1	1		4		
	4				1				1	
Microcytherura angulosa	A	17	15	57	30	34	70	38	24	23
	1	2	4	13	18	14	18	7	8	
Neonesidea mediterranea	A			3	1	1	2	1	1	1
	1		2	2	1		2			
	2	1	3		4		3	1		2
	3		2		1					
	4		2	5	3	3	5	2		
	5	1	2	7		5	3	2	1	1
	6		4	2	1	1	4	3	3	3
	7	1		9	2	3		1	1	2
Paracytheridea triquetra	A	1	2	3	5	2	1	2	1	
	1	1	1	2			3	2	3	
	2	1	1	4	2	2	6	1	1	
	3	2	1	2		3	1	2		1
Semicytherura acuticostata	A	2	7	10	6	11	12	7	8	2
Semicytherura alifera	A	8	6	19	9	12	23	11	9	3
	1					1				
Semicytherura rara	A			1		2	1			
Xestoleberis communis	A	3	4			1		6	1	
	1		2	2	1	1	1		1	1
	2	3	10	10	9	2	16	5	4	5
	3	10	6	6	5	1	12	4	8	1
	4	1		3			1	1		1
Xestoleberis dispar	A	1	2	6	3	5	4	2	1	1
	1	2		1	4	3	1	1		1
	2	1	2	3	5	3	2	1	1	2
	3					2	2		2	
Xestoleberis plana + aff. *perula*	A									1
	1			2	2					
	2			1						
	3				1	3		2	1	1

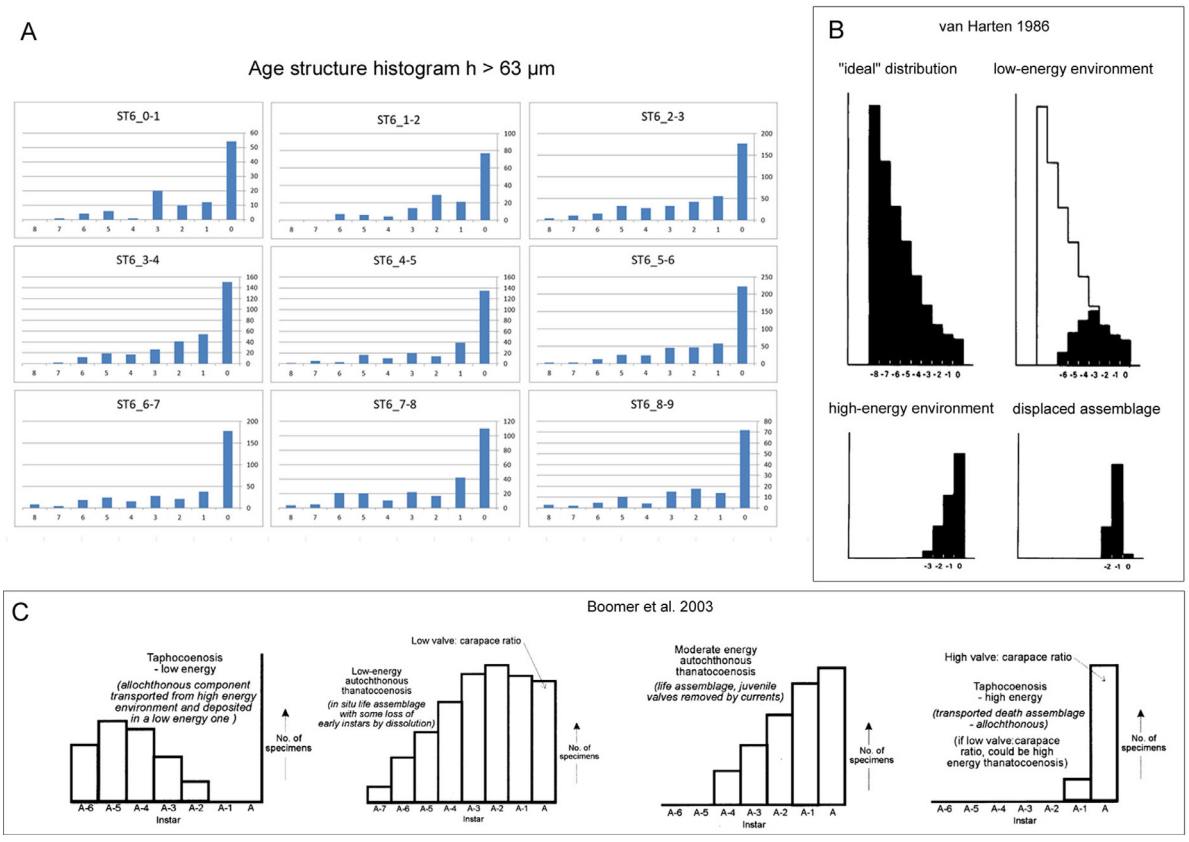

Fig. 13. Comparison between different methods to assess Population Age Structure. A) Assemblage Population Age Structure histograms calculated for *h* >63 µm (0 corresponds to adults and 1–8 to development stages); B) The four "schematic population structures" defined by van Harten (1986) for "ideal," low-energy, high-energy and displaced assemblages; C) The four histograms proposed by Boomer at al. (2003).

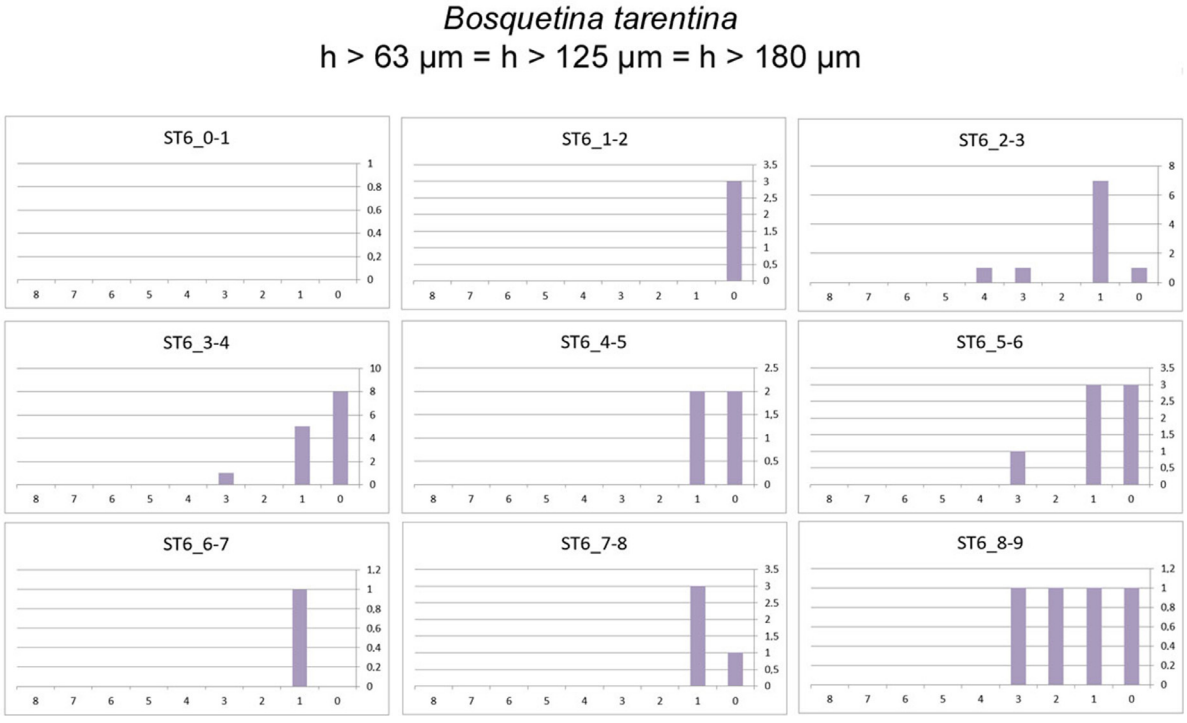

Fig. 14. *Bosquetina tarentina* specific Population Age Structure histograms. The histograms for *h* >63 µm are the same as *h* >125 µm and *h* >180 µm; 0 corresponds to adults and 1–8 to development stages.

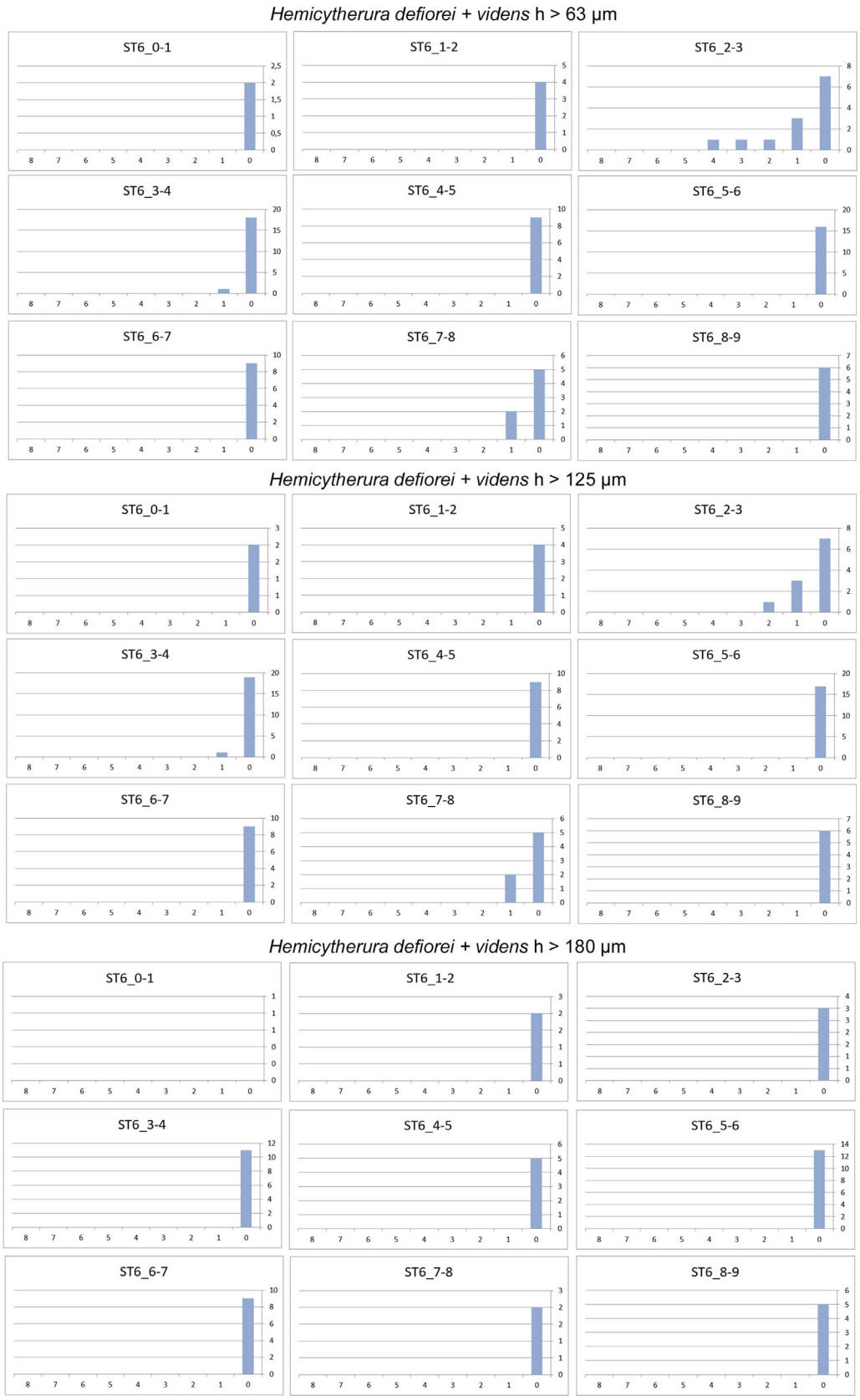

Fig. 15. *Hemicytherura defiorei + videns* specific Population Age Structure histograms for *h* >63 µm, *h* >125 µm and *h* >180 µm; 0 corresponds to adults and 1–8 to development stages.

B2, except *Cytherella vulgatella* and *Bosquetina tarentina* (autochthonous). Cluster B1 consists of autochthonous species (*Hemicytherura defiorei + videns, Microcythere depressa, hians, inflexa, Microcytherura angulosa, Semicytherura acuticostata, alifera, rara*) with high values of SPS (SPSm >7).

In the Principal Cluster Analysis (PCA) performed on valves with *h* >63 μm (Fig. 8), the first axis explains 60.6% of the variance of data (eigenvalue = 21.2). The second axis accounts for 15.3% of the variance (eigenvalue = 5.3). The species characterized by high SPS values and considered as entirely autochthonous based on distribution data (*Hemicytherura defiorei + videns, Microcythere depressa, hians, inflexa, Microcytherura angulosa, Semicytherura acuticostata, alifera, rara*) are grouped in the right part of the diagram, near the first axis. This group corresponds to the species forming the cluster B1 (Fig. 7).

Cluster analysis conducted on valves with *h* >125 μm (Fig. 9) yields two clusters, *α* and *β*. The former consists of two small autochthonous species, *Microcytherura depressa* and *Microcytherura hians*; the latter can be divided into three subclusters (*β*1, *β*2 and *β*3). The subcluster *β*2 consists of five autochthonous species: *Hemicytherura defiorei + videns, Microcytherura angulosa, Semicytherura acuticostata, alifera, rara*).

The diagram of PCA *h* >125 μm (Fig. 10) (first axis explains 64.1% of the variance of data, eigenvalue = 35.1; second axis accounts for 12.0% of the variance, eigenvalue = 6.6) groups the five species forming subcluster *β*2 in its right part, near the first axis.

Both Cluster analysis and PCA (first axis explains 62.2% of the variance of data, eigenvalue = 32.2; second axis accounts for 12.9% of the variance, eigenvalue = 6.7) performed on valves with *h* >180 μm (Figs. 11, 12) do not yield results that are well related with the hypothesized autochthoneity-allochthoneity of the considered species. In fact, the analyses grouped together *in situ* and displaced taxa, and are, in our opinion, inconclusive to describe the autochthoneity/allochthoneity trends.

4. Discussion

Ostracod shells are characterized by features (delicate ornaments, transparent valves) that frequently allow the discrimination, in mixed assemblages, between autochthonous and transported taxa, based on qualitative assessment of the state of preservation. In some cases, both in fossil and modern assemblages, the discrimination between autochthonous and allochthonous forms is not obvious. The characteristics of the ostracod assemblages of the circalittoral samples collected in the vicinity of the Zannone Giant Pockmark, in the Tyrrhenian Sea (Aiello et al., 2022), suggested the presence of transported shells, due to downslope contamination. There is no evidence of reworked (i.e., derived from older sediments) specimens. Dominant and characteristic species pertain both to genera commonly recorded in the circalittoral waters of the Mediterranean, such as *Callistocythere* and *Semicytherura*, and to species of *Microcythere* and *Microcytherura*, usually underestimated because of their small dimensions. Three groups of species, namely autochthonous, allochthonous, and present with both *in situ* and transported valves, have been hypothesized on the basis of distribution data and qualitative assessment of the population age structure (Table 7). The quantitative analyses performed herein represent an attempt to evaluate the accuracy of previously proposed methods aimed at distinguishing auto-allochthoneity in this case.

The environment where the examined samples were collected, at 127 m bsl on the Zannone insular shelf, can be compared to the "fine grain, low energy" outer sublittoral depth zone (100–200 m bsl) identified by Brouwers (1988) in the Gulf of Alaska shelf. As shown in Table 3, the A:J values recorded in the Pontine Shelf ranging from 0.71 to 1.65 are consistently higher than the corresponding Alaskan "outer sublittoral" ratios (average A:J ratio = 0.65; Brouwers, 1988, p. 236). In contrast, our values are similar to those reported by Brouwers for the upper part (50–60 m bsl) of the "middle sublittoral depth zone," where the A:J ratio ranges from 0.94 to 1.37. Consequently, we suggest that the use of A:J ratio as paleobathymetric tool in paleoenvironmental studies must be considered with caution.

The methodological approach based on Population Age Structure proposed by Whatley (1983, 1988), van Harten (1986) and Boomer et al. (2003) uses quantitative data (number of valves pertaining to different stages) in order to build PAS histograms, whereas the comparison between different assemblages is at least partly qualitative. The PAS histograms of the nine subsamples of the ST6_BNR1 short core do not show any similarity with the four "schematic population structures" defined by van Harten (1986) for "ideal" low-energy, high-energy and displaced assemblages (Fig. 13). Conversely, they fit well, both for *h* >63 μm, *h* >125 μm and *h* >180 μm histograms (Figs. 4, 13), with the "moderate energy autochthonous thanatocoenosis" of Boomer et al. (2003), representing "life assemblage" with young instars removed by currents. In the Zannone assemblages, the stages A-5 and A-6, lacking in the cited studies (Whatley, 1983, 1988; van Harten, 1986; Boomer et al., 2003) are present, suggesting a low water energy. We have attempted to extend the comparison of the different PAS of Boomer et al. (2003) with the PAS histograms of the most abundant species. For example, the PAS of *Microcytherura angulosa* (Fig. 5) is comparable with the "moderate energy autochthonous thanatocoenosis", whereas the "disordered" population age structures of *Neonesidea mediterranea* (Fig. 6) is relatively similar to the "Taphocoenosis" histograms, with allochthonous shells transported from high energy environment into low energy one (Boomer et al., 2003). The hypothesized autochthoneity of *Microcytherura angulosa* and the allochthoneity of *Neonesidea mediterranea* seems confirmed. Clearly this method can be used only for forms represented by some tens of specimens, and not for accessory (*e.g., Bosquetina tarentina*, Fig. 14) and uncommon species. Results are not relevant for small sized species due to the rarity of young instars (*e.g., Hemicytherura defiorei + videns*, Fig. 15).

Analyses performed on Specific Population Stage (SPS) have, in our opinion, the potential to be an effective tool in distinguishing between autochthonous and allochthonous taxa in modern and fossil assemblages. Both Cluster analysis and PCA (*h* >63 μm) reveal distinct group of entirely autochthonous species including *Hemicytherura defiorei + videns, Microcythere depressa, Microcythere hians, Microcythere inflexa, Microcytherura angulosa, Semicytherura acuticostata, Semicytherura alifera, Semicytherura rara*, and groups of transported species. The proposed analyses based on SPS display a high paleoecological value, due to the ability to discern which taxa might best support paleoenvironmental interpretations.

5. Conclusions

Here we utilize nine subsamples from a short sediment core to directly assess the autochthoneity of the dead ostracod assemblage. An ostracod death assemblage should retain a long-term record composed by both juvenile and adult stages. The preservation potential of the ostracod calcitic shell in marine environments is high, as is their potential to be transported in excellent preservation. This presents both opportunities and constraints in that the death assemblage may record recent occupation or occupation in a more distant past, the latter of which no longer maps the extent of the present-day living community, but also transport dynamics that would otherwise be difficult to detect in the sediment record. Before applying the SPS method, the preservation of the assemblage should be analysed as well as potential diagenetic impacts, linked to chemical changes and different lithologies. Through the revision of the distribution data reported in classic and modern literature on Mediterranean ostracods, we compiled a list of putative *in situ* and displaced ostracod species. Then we tested the hypothesis against statistical analyses of the population structure using the new SPS index on three different grain sizes.

The analyses presented here suggest that the analysis on the small grain size (*h* >63 μm) is the most effective in describing the putative living ostracod population in a modern assem-

blage, and thus in describing the paleoenvironment. Tiny species (such as *Microcythere depressa, Microcythere angulosa*) are generally under-represented in the fossil record of the Mediterranean probably due to sample processing bias and not to the rarity of the species itself. Assessing the autochthoneity of modern/fossil assemblages has great potential for acquiring baseline information on ecosystems before the onset of human activities. Furthermore, defining the autochthoneity of modern/fossil assemblage improves the definition of paleoenvironmental and paleobathymetric reconstructions which could be biased by displaced/reworked specimens.

Declaration of Competing Interest

The authors declare that they have no known competing financial interests or personal relationships that could have appeared to influence the work reported in this paper.

Data availability

Data will be made available on request.

Acknowledgements

We would like to thank Letizia Di Bella (Sapienza University of Rome) and Michela Ingrassia (CNR-IGAG) for making available the samples from ST6_BNR1 and for providing site information. We thank Alan Lord and Ian Boomer for their reviews that greatly improved the manuscript.

Appendix 1

List of species

Argilloecia caudata Müller, 1894
Argilloecia robusta Bonaduce et al., 1976
Aurila convexa (Baird, 1850)
Aurila interpretis Uliczny, 1969
Aurila speyeri (Brady, 1858)
Bosquetina tarentina (Baird, 1850)
Buntonia sublatissima (Neviani, 1906)
Bythocythere puncticulata Ruggieri, 1976
Callistocythere crispata (Brady, 1868)
Callistocythere flavidofusca (Ruggieri, 1950)
Callistocythere praecincta Ciampo, 1976
Carinocythereis carinata (Roemer, 1838)
Carinocythereis whitei (Baird, 1850)
Cistacythereis turbida (Müller, 1894)
Cluthia keiji Neale, 1975
Costa edwardsii (Roemer, 1838)
Cytherella vulgatella Aiello, Barra, Bonaduce and Russo, 1996
Cytherois frequens Müller, 1894
Cytherois uffenordei Ruggieri, 1975
Cytheropteron hadriaticum Bonaduce et al., 1976
Cytheropteron latum Müller, 1894
Cytheropteron sulcatum Bonaduce et al., 1976
Dopseucythere mediterranea (Bonaduce, Masoli, Pugliese and McKenzie, 1980)
Echinocythereis laticarina (Brady, 1868)
Eucythere curta Ruggieri, 1975
Eucytherura complexa (Brady, 1867)
Eucytherura gibbera Müller, 1894
Eucytherura mistrettai Sissingh, 1972
Hemicytherura defiorei Ruggieri, 1953
Hemicytherura videns (Müller, 1894)
Hernryhowella partenopea Bonaduce, Barra and Aiello,1999
Kangarina abyssicola (Müller, 1894)
Loxocauda decipiens (Müller, 1894)
Loxoconcha affinis (Brady, 1866)
Loxoconcha ovulata (Costa, 1853)
Loxoconcha stellifera Müller, 1894
Microcythere depressa Müller, 1894
Microcythere hians Müller, 1894
Microcythere inflexa Müller, 1894
Microcytherura angulosa (Seguenza, 1880)
Microcytherura nigrescens Müller, 1894
Microxestoleberis kikladica Barbeito-Gonzalez, 1971
Microxestoleberis nana Müller, 1894
Microxestoleberis xenomys (Barbeito-Gonzalez, 1971)
Microxestoleberis sp.
Monoceratina oblita Bonaduce et al., 1976
Neonesidea formosa (Brady, 1868)
Neonesidea mediterranea (Müller, 1894)
Occultocythereis dohrni Puri, 1963
Paracytheridea triquetra (Reuss, 1850)
Paracytherois flexuosa (Brady, 1867)
Paracytherois oblonga Müller, 1894
Paracytheromorpha nana (Bonaduce et al., 1976)
Paracytheromorpha sp.
Paradoxostoma simile Müller, 1894
Paranesidea reticulata (Müller, 1894)
Phlyctocythere pellucida (Müller, 1894)
Polycope reticulata Müller, 1894
Pontocypris acuminata (Müller, 1894)
Pontocythere turbida (Müller, 1894)
Propontocypris dispar (Müller, 1894)
Prontocypris intermedia (Brady, 1868)
Propontocypris pirifera (Müller, 1894)
Pseudocytherura strangulata Ruggieri, 1991
Pterygocythereis jonesii (Baird, 1850)
Pterygocythereis coronata (Roemer, 1838)
Sclerochilus aequus Müller, 1894
Semicytherura acuticostata (Sars, 1866)
Semicytherura aenariensis Bonaduce et al., 1976
Semicytherura alifera Ruggieri, 1959
Semicytherura dispar (Müller, 1894)
Semicytherura heinzei Puri, 1963
Semicytherura inversa (Seguenza, 1880)
Semicytherura paradoxa (Müller, 1894)
Semicytherura quadridentata (Hartmann, 1953)
Semicytherura rara (Müller, 1894)
Semicytherura simplex (Brady and Norman, 1889)
Tenedocythere prava (Baird, 1850)
Urocythereis ilariae Aiello, Barra and Parisi, 2016
Urocythereis margaritifera (Müller, 1894)
Xestoleberis communis Müller, 1894
Xestoleberis dispar Müller, 1894
Xestoleberis plana Müller, 1894
Xestoleberis aff. *intumescens* Klie, 1942
Xestoleberis aff. *perula* Athersuch, 1978

References

Aiello, G., Barra, D., Coppa, M.G., Valente, A., Zeni, F., 2006. Recent infralittoral foraminiferida and Ostracoda from the porto cesareo lagoon (Ionian Sea, Mediterranean). Boll. Soc. Paleontol. Ital. 45 (1), 1–14.

Aiello, G., Barra, D., 2010. Crustacea, Ostracoda. Biologia Marina Mediterranea 17 (1), 401–419. doi:10.1093/oso/9780199233267.003.0025, Supplement.

Aiello, G., Barra, D., Parisi, R., Isaia, R., Marturano, A., 2018. Holocene benthic foraminiferal and ostracod assemblages in a paleo-hydrothermal vent system of Campi Flegrei (Campania, South Italy). Palaeontologia Electronica 21 (3), 1–71. doi:10.26879/835.

Aiello, G., Barra, D., Parisi, R., Arienzo, M., Donadio, C., Ferrara, L., Toscanesi, M., Trifuoggi, M., 2021. Infralittoral Ostracoda and benthic foraminifera of the Gulf of Pozzuoli (Tyrrhenian Sea, Italy). Aquat. Ecol. 55, 955–998. doi:10.1007/s10452-021-09874-1.

Aiello, G., Mazzini, I., Parisi, R., Ingrassia, M., Barra, D., 2022. Are CO2 rich sea-floor pockmarks a suitable environment for ostracod assemblages? The example of the

Zannone Giant Pockmark (central-eastern Tyrrhenian). Mar. Ecol. e12698, 1–32. doi:10.1111/maec.12698.

Balassone, G., Aiello, G., Barra, D., Cappelletti, P., De Bonis, A., Donadio, C., Guida, M., Melluso, L., Morra, V., Parisi, R., Pennetta, M., Siciliano, A., 2016. Effects of anthropogenic activities in a Mediterranean coastland: the case study of the Falerno-Domitio littoral in Campania, Tyrrhenian Sea (southern Italy). Mar. Pollut. Bull. 112, 271–290. doi:10.1016/j.marpolbul.2016.08.004.

Barbeito-Gonzalez, P.J., 1971. Die Ostracoden des Küstenbereiches von Naxos (Griechenland) und ihre Lebensbereiche. Mitteilungen aus dem hamburgischen zoologischen Museum und Institut 67, 255–326.

Blachowiak-Samolyk, K., Angel, M.V., 2007. A year round comparative studies on the population structures of pelagic Ostracoda in the Admiralty Bay (Southern Ocean). Hydrobiologia 585, 67–77. doi:10.1007/s10750-007-0629-2.

Bonaduce, G., Ciampo, G., Masoli, M., 1976. Distribution of Ostracoda in the Adriatic sea. Pubbl. Stazione Zool. Napoli 40 (1), 1–304 supplemento.

Bonaduce, G., Masoli, M., Pugliese, N., 1977. Ostracodi bentonici dell'alto Tirreno. Studi Trent. Sci. Nat. Acta Biol. 54, 243–261.

Boomer, I., Horne, D.J., Slipper, I.J., 2003. The use of ostracods in palaeoenvironmental studies, or what can you do with an ostracod shell? In: Park, L.E., Smith, A.J. (Eds.) Bridging the Gap: Trends in the Ostracode Biological and Geological Sciences. The Paleontological Society, pp. 153–179. doi:10.1017/S1089332600002199 Papers 9.

Breman, E., 1976. The Distribution of Ostracodes in the Bottom Sediments of the Adriatic Sea Academisch Proefschrift. Vrije Universiteit te Amsterdam, Amsterdam, p. 165.

Brouwers, E.M., 1988. Sediment transport detected from analysis of ostracod population structure: an example from the Alaska continental shelf. In: de Deckker, P., Colin, J.P., Peypouquet, J.P. (Eds.), Ostracoda in the Earth Sciences. Elsevier, pp. 231–244.

Danielopol, D.L., Ito, E., Wansard, G., Kamiya, T., Cronin, T.M., Baltanás, A., 2002. Techniques for collection and study of Ostracoda. In: The Ostracoda: Applications in Quaternary Research, Geophysical Monograph 131. American Geophysical Union, pp. 65–98. doi:10.1029/131GM04.

Danielopol, D.L., Baltanás, A., Namiotko, T., Geiger, W., Pichler, M., Reina, M., Roidmayr, G., 2008. Developmental trajectories in geographically separated populations of non-marine ostracods: morphometric applications for palaeoecological studies. Senckenbergiana Lethaea 88 (1), 183–193. doi:10.1007/BF03043988.

De Deckker, P., 2002. Ostracod palaeoecology. In: The Ostracoda: Applications in Quaternary research. AGU Geophysical Monograph Series 131, pp. 121–134. doi:10.1029/131GM06.

Di Bella, L., Ingrassia, M., Frezza, V., Chiocci, F.L., Martorelli, E., 2016. The response of benthic meiofauna to hydrothermal emissions in the Pontine Archipelago, Tyrrhenian Sea (central Mediterranean Basin). J. Mar. Syst. 164, 53–66. doi:10.1016/j.jmarsys.2016.08.002.

Dillon, E.M., Pier, J.Q., Smith, J.A., Raja, N.B., Dimitrijević, D., Austin, E.L., Cybulski, J.D., De Entrambasaguas, J., Durham, S.R., Grether, C.M., Haldar, H.S., 2022. What is conservation paleobiology? Tracking 20 years of research and development. Front. Ecol. Evol. 10, 1031483.

do Carmo, D.A., Whatley, R.C., Timberlake, S., 1999. Variable noding and palaeoecology of a Middle Jurassic limnocytherid ostracod: implications for modern brackish water taxa. Palaeogeogr. Palaeoclimatol. Palaeoecol. 148 (1–3), 23–35. doi:10.1016/S0031-0182(98)00173-4.

Fagerstrom, J.A., 1964. Fossil communities in paleoecology: their recognition and significance. Geol. Soc. Am. Bull. 75, 1197–1216. doi:10.1130/0016-7606(1964)75[1197:FCIPTR]2.0.CO;2.

Fontana, S.L., Ballent, S., 2005. A new giant cypridid ostracod (Crustacea) from southern Buenos Aires Province, Argentina. Hydrobiologia 533, 187–197. doi:10.1007/s10750-004-2415-8.

Gibbard, P.L., Head, M.J., 2020. Chapter 30 - the quaternary period. Geol. Time Scale 2020, 1217–1255. doi:10.1016/B978-0-12-824360-2.00030-9.

Hammer, Ø., Harper, D.A.T., Ryan, P.D., 2001. PAST: paleontological statistics software package for education and data analysis. Palaeontologia Electronica 4 (1).

Hoehle, M., Wrozyna, C., 2022. Spatio-temporal distribution of ostracod species in saline inland lakes (Mansfeld lake area; Central Germany). PeerJ 10, e13668. doi:10.7717/peerj.13668.

Horne, D.J., Cabral, M.C., Fatela, F., Radl, M., 2021. Salt marsh ostracods on European Atlantic and North Sea coasts: aspects of macroecology, palaeoecology, biogeography, macroevolution and conservation. Mar. Micropaleontol. 174, 101975.

Ingrassia, M., Martorelli, E., Bosman, A., Macelloni, L., Sposato, A., Chiocci, F.L., 2015. The Zannone Giant Pockmark: first evidence of a giant complex seeping structure in shallow-water, central Mediterranean Sea, Italy. Mar. Geol. 363, 3–51. doi:10.1016/j.margeo.2015.02.005.

Kidwell, S.M., 2007. Discordance between living and death assemblages as evidence for anthropogenic ecological change. Proc. Natl Acad. Sci. 104 (45), 17701–17706.

Kock, R., 1992. Ostracods in the epipelagial zone off the Antarctic Peninsula - a contribution to the systematics and to their distribution and population structure with regard to seasonality. Berichte zur Polar- und Meeresforschung 106, 1–209.

Mangoni, O., Aiello, G., Balbi, S., Barra, D., Bolinesi, F., Donadio, C., Ferrara, L., Guida, M., Parisi, R., Pennetta, M., Trifuoggi, M., Arienzo, M., 2016. A multidisciplinary approach for the characterization of the coastal marine ecosystems of Monte Di Procida (Campania, Italy). Mar. Pollut. Bull. 112, 443–451. doi:10.1016/j.marpolbul.2016.07.008.

Müller, G.W., 1894. Die Ostracoden des Golfes von Neapel und der angrenzenden Meeres-Abschnitte. Fauna und Flora des Golfes von Neapel und der angrenzenden Meeres-Abschnitte. Herausgegeben von der Zoologischen Station zu Neapel 21 (1–8), 404.

Mao, X., Liu, X., Li, J., Feng, S., Jiang, G., Liu, L., 2021. Population age structure of ostracods in lake sediment and its implication for within-lake transport of microfossils. Ecol. Indic. 131, 108182. doi:10.1016/j.ecolind.2021.108182.

Marin, V., 1987. The oceanographic structure of the eastern Scotia sea-IV. Distribution of copepod species in relation to hydrography in 1981. Deep Sea Research Part A. Oceanogr. Res. Pap. 34 (1), 105–121. doi:10.1016/0198-0149(87)90125-7.

Ruiz, F., González-Regalado, M.L., Muñoz, J.M., 1997. Multivariate analysis applied to total and living fauna: seasonal ecology of recent benthic Ostracoda off the North Cádiz Gulf coast (southwestern Spain). Mar. Micropaleontol. 31 (3–4), 183–203. doi:10.1016/S0377-8398(96)00060-6.

Ruiz, F., González-Regalado, M.L., Muñoz, J.M., Pendón, J.G., Rodríguez-Ramírez, A., Cáceres, L., Rodríguez Vidal, J., 2003. Population age structure techniques and ostracods: applications in coastal hydrodynamics and paleoenvironmental analysis. Palaeogeogr. Palaeoclimatol. Palaeoecol. 199, 51–69. doi:10.1016/S0031-0182(03)00485-1.

Uffenorde, H., 1972. Oekologie und jahreszeitliche Verteilung rezenter bentonischer Ostracoden des Limski kanal bei Rovinj (nördliche Adria). Göttinger Arbeiten zur Geologie und Paläontologie 13, 1–121.

van Harten, D., 1986. Use of ostracodes to recognize downslope contamination in paleobathymetry and a preliminary reappraisal of the paleodepth of the Prasas Marls (Pliocene), Crete, Greece. Geology 14 (10), 856–859. doi:10.1130/0091-7613(1986)14⟨856:UOOTRD⟩2.0.CO;2, October 1986.

Whatley, R.C., 1983. Some simple procedures for enhancing the use of Ostracoda in palaeoenvironmental analysis. Norwegian Petroleum Directorate. Bulletin 2, 129–146.

Whatley, R.C., 1988. Population structure of ostracods: some general principles for the recognition of palaeoenvironments. In: De Deccker, P., Colin, J.P., Peypouquet, J.P. (Eds.), Ostracoda in the Earth Sciences. Elsevier, Amsterdam, pp. 245–256.

Zhai, D., Xiao, J., Fan, J., Wen, R., Pang, Q., 2015. Differential transport and preservation of the instars of *Limnocythere inopinata* (Crustacea, Ostracoda) in three large brackish lakes in northern China. Hydrobiologia 747 (1), 1–18. doi:10.1007/s10750-014-2118-8.

Zhai, D., Xiao, J., Fan, J., Zhou, L., Wen, R., Pang, Q., 2013. Spatial heterogeneity of the population age structure of the ostracode *Limnocythere inopinata* in Hulun Lake, Inner Mongolia and its implications. Hydrobiologia 716 (1), 29–46. doi:10.1007/s10750-013-1541-6.